

Soft Bio-Microrobots: Toward Biomedical Applications

Zihan Wang, Anke Klingner, Veronika Magdanz, Sarthak Misra,
and Islam S. M. Khalil*

Soft bio-microrobots have the potential to execute complex tasks in unexpected and harsh environments of the human body due to their dexterity and flexibility. The architectural designs of soft bio-microrobots either replicate the motion of natural creatures or capitalize on their motility. Based on this design principle, biologically inspired microrobots that imitate the movements and functions of biological systems, such as starfish, bacteria, and sperm cells, as well as bio-hybrid microrobots that combine motile micro-organisms or cells with functional components have been developed. Herein, an overview of the design principles, energy sources, and biomedical applications of existing soft bio-microrobots is presented. It is shown that the incorporation of externally responsive material enables biologically inspired microrobots to change their shapes and imitate the motion of living organisms under external stimuli, and it is interpreted how biohybrid microrobots are guided through the tactic behavior of microorganisms or cells. Finally, perspectives on key challenges that soft bio-microrobots must overcome to achieve in vivo biomedical applications are given.

interest in both research and industrial fields, including deep-sea exploration,^[2] underwater investigation,^[3] and surgery.^[4] Unlike rigid-linked robots, soft robots are made of flexible or extensible materials and can deform in reaction to stimuli. These flexible or extensible materials would undergo continuous deformation when exposed to external fields, such as magnetic,^[5,6] light,^[7,8] electric,^[9,10] and acoustic fields.^[11,12] This feature can be harnessed to achieve locomotion or manipulation, imparting versatility and multifunctionality to soft robots. Moreover, the compliance of soft robots allows them to conform to complex or irregular shapes. Consequently, soft robots can interact with their surroundings, providing a unique advantage for a wide range of applications that necessitate a high degree of dexterity and flexibility.

The property of compliance and flexibility will likely enhance the capabilities of robots irrespective to scale. The miniaturization of soft robots can open up a new avenue for microscale manipulation.

The size limitations of large soft robots pose challenges in surgical applications, as they are unsuitable for use in confined spaces. Developing soft microrobots that can be deployed in compact spaces or hard-to-reach positions is crucial. Microrobots, unlike macroscale robots powered by batteries, must adopt offboard power. This is because the power of onboard batteries drastically attenuates with the volume. When the size of robots is reduced to micro/nanometers, the inertial force is dominated by the viscous force, which is the so-called low-Reynolds (Re) number regime.^[13] Our intuition built in the macroworld is not applicable to microrobots. The reciprocal motion of microrobots will lead to no net displacement. To move in low Re, the body configuration of microrobots must break time reversibility. In nature, many microorganisms provide us with the cue to achieve movement in low Re. The whip-like motion of the flagellum allows microorganisms to move forward.^[14] For instance, the green algae, *Chlamydomonas reinhardtii*, is a two-flagellated microorganism that can display ciliary and flagellar beat patterns.^[15] As a typical puller, it relies on two synchronized flagella in the front to push the fluid backward and pull the cell body forward. On the contrary, spermatozoa have their flagellum in the back and the passive head in the front, forming propagating waves backward, pushing the cell body to move.^[16] The design of soft bio-microrobots has been greatly influenced by this flagellum-like motion.

Emulating the motion of microorganisms can enable soft bio-microrobots to break the time reversibility and propel in

1. Introduction


Soft robots, created with customized compliant elements integrated into mechanical structures, have made a significant impact in practical applications.^[1] They have attracted extensive

Z. Wang, S. Misra
Department of Biomedical Engineering
University of Groningen and University Medical Center Groningen
9713 GZ Groningen, The Netherlands

A. Klingner
Department of Physics
The German University in Cairo
New Cairo 11835, Egypt

V. Magdanz
Department of Systems Design Engineering
University of Waterloo
200 University Ave W, Waterloo, Ontario N2L3G1, Canada

S. Misra, I. S. M. Khalil
Department of Biomechanical Engineering
University of Twente
7500 AE Enschede, The Netherlands
E-mail: i.s.m.khalil@utwente.nl

 The ORCID identification number(s) for the author(s) of this article can be found under <https://doi.org/10.1002/aisy.202300093>.

© 2023 The Authors. Advanced Intelligent Systems published by Wiley-VCH GmbH. This is an open access article under the terms of the Creative Commons Attribution License, which permits use, distribution and reproduction in any medium, provided the original work is properly cited.

DOI: 10.1002/aisy.202300093

low Re. To this end, the fabrication of soft bio-microrobots necessitates the use of soft and flexible materials that can be difficult to work with conventional fabrication methods. Recently, 3D printing,^[17,18] soft lithography,^[19,20] electrodeposition,^[21,22] biotemplated synthesis,^[23–25] and lamination methods^[26] have been utilized to fabricate biomimetic soft microrobots. Soft microrobots composed of multiple segments can be produced through the electrodeposition of soft and rigid materials, and they can exhibit flagellum-like motion in response to external stimuli. The cyclic rotation of the externally responsive segment causes the nonresponsive segment to rotate at different amplitudes, leading to nonreciprocal motion. Owing to their soft flagella, microorganisms and cells, such as sperm,^[27] bacteria,^[28] and algae,^[29] can supply the required mobility for soft bio-microrobots. The integration of motile microorganisms or cells with functional components creates soft microrobots with the ability to move and serve desired biomedical purposes. The inspiration from nature has been effectively incorporated into the design of soft bio-microrobots, promoting the development of soft bio-microrobots.^[30]

In this review, some relevant examples will be given to summarize the development of soft bio-microrobots, including their design principles, energy sources, and biomedical applications (see Figure 1). We first discuss the design principles in

Section 2. Since biomimetics is the primary design methodology for soft bio-microrobots, they can be divided into two types: biologically inspired and biohybrid microrobots. Biologically inspired microrobots encompass microrobots with joints, microrobots with soft segments, and microrobots with soft and continuous bodies inspired by spermatozoa (Figure 1A), while biohybrid microrobots include sperm-based microrobots, bacteria-driven microrobots, and algal microrobots (Figure 1B). The fabrication method, materials, and actuation methodology are discussed for each example of soft bio-microrobots. The energy sources of soft bio-microrobots include magnetic, acoustic, optical, and chemical power (Figure 1C,D,E,F), which is discussed in Section 3. Catalytic micromotors, which achieve propulsion by means of chemical energy produced in catalytic reaction, are out of the scope of soft and flexible bio-microrobots. The term “chemical energy (power)” refers to the energy converted in the metabolic process of microorganisms or cells throughout this text. The energy is ultimately transformed into kinetic energy of soft bio-microrobots. Soft bio-microrobots are able to acquire propulsion by flagellum mimicking or flagellar beating. In the presence of external fields, the flexible component of soft bio-microrobots can respond to them and mimic the flagellar beating, thereby generating movement. Microorganisms and cells with

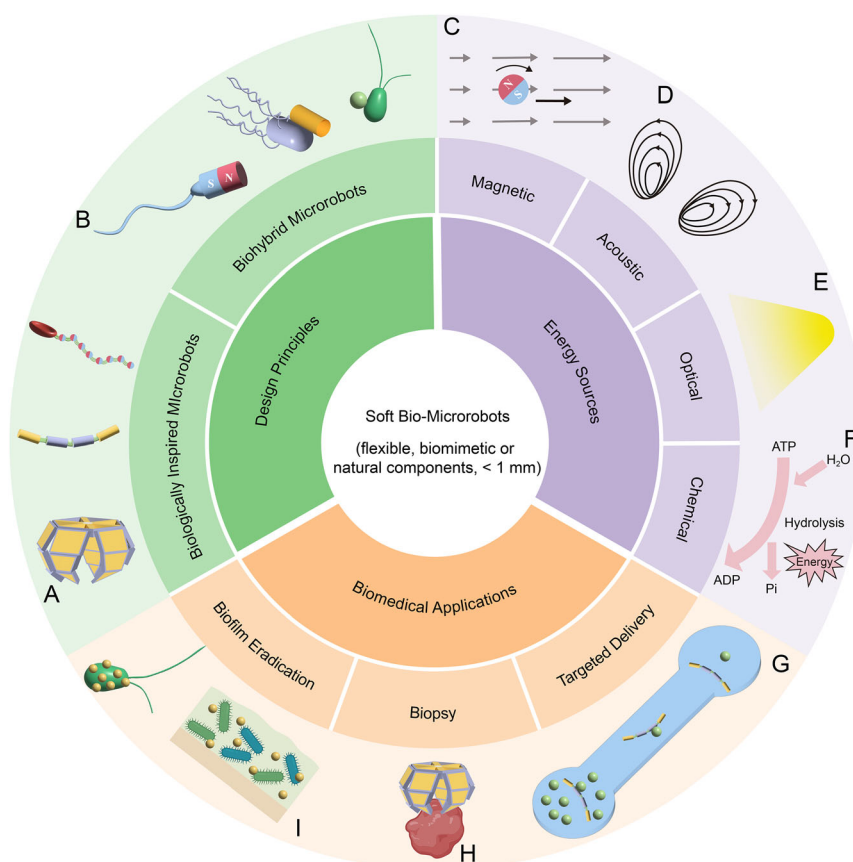


Figure 1. Schematic illustration of soft bio-microrobots, including their design principles, energy sources, and biomedical applications. Biologically inspired design results in (A) microrobots with joints, flexible segments, and continuous bodies. Biohybrid microrobots are created through (B) sperm-, bacteria-, and algae-driven mechanisms. The energy sources, including (C) magnetic, (D) acoustic, (E) optical, and (F) chemical power, are used to actuate soft bio-microrobots. The biomedical applications encompass (G) targeted delivery, (H) biopsy, and (I) biofilm eradication.

deformable flagella can be combined with functional materials through physical binding or chemical bonding, providing motility for soft bio-microrobots. External stimuli such as oxygen, pressure, chemicals, magnetic field, light, and temperature changes are essential cues for microorganisms or cells to find food, avoid harmful environments, and interact with surrounding environments. These inherent tactic behaviors of microorganisms and cells ease the directional control of biohybrid microrobots. Section 4 introduces and generalizes biomedical applications of soft bio-microrobots in three aspects, including targeted delivery (Figure 1G), biopsy (Figure 1H), and biofilm removal (Figure 1I). In the last section, we give our insights and reveal the confronting challenges in the realm of soft bio-microrobots.

2. Design Principles of Soft Bio-Microrobots

Soft bio-microrobots are often created with designs inspired by living organisms or utilizing microorganisms and cells capable of swimming to produce thrust. Nature has provided several sources of inspiration for the development of soft bio-microrobots. The main fabrication methodology of soft bio-microrobots is based on biomimetics, which guides us in replicating living organisms and constructing similar designs. Biologically inspired microrobots can exhibit movements similar to those of living organisms under external stimuli. Conversely, biohybrid microrobots have biological microorganisms or cells integrated as the power sources, structural units, or loading entities. With simple modifications to biomedical materials, they are capable of performing biomedical tasks.^[31] In summary, biologically inspired microrobots imitate microorganisms to obtain motility, whereas biohybrid microrobots rely on the inherent motility of microorganisms or cells.

2.1. Biologically Inspired Microrobots

Biologically inspired microrobots refer to soft microrobots replicating the motion and function of living organisms. During microrobots fabrication, soft materials are utilized to facilitate the deformation of their bodies, mimicking the movement or manipulation of living organisms. For example, microgrippers with flexible joints imitate human hands and complete the task of grasping. **Figure 2A** displays that a microgripper grips like a human fist when the residual stress is released by the trigger of chemicals or temperature. Moreover, the flexibility of soft segments permits deformation in response to external stimuli, thereby enabling microrobots to replicate the swimming strategy of microorganisms that are propelled by flagella (see **Figure 2B**). Biologically inspired structures, such as flexible joints, soft segments, and soft continuous bodies, empower microrobots to achieve similar functionality to living organisms.

2.1.1. Microrobots with Joints

Flexible joints are able to improve the agility of robots when executing complex manipulations. In the presence of joints, human hands can bend at interphalangeal joints and grasp objects. Through the coordination of joints in each finger, the human hand can grip and unfold to perform pick-and-place. Grippers,

which can pick and place objects, are a typical example inspired by the human hand. Conventional grippers are usually tethered to electric cables or pneumatic tubes, which regulate the actuation and operation. However, these tethers restrict the miniaturization and maneuverability of the grippers. The emergence of untethered microgrippers can address these problems and offer a way for manipulating individual cells, and microbes, and carrying out targeted cell examination and evaluation.^[32,33]

Randhawa and co-workers have fabricated mobile microgrippers based on microelectromechanical systems techniques.^[34] The microgripper comprises trilayer joints capable of gripping after releasing residual stress of the chromium/copper metallic bilayer, as shown in **Figure 2C**. Once the microgripper is detached from the substrate, the residual stress is released, the supportive layer maintains the microgripper open. Gripping can be triggered after dissolving the supportive layer. The incorporation of magnetic materials, such as nickel and iron, enables the microgrippers to move with a magnet. By replacing the supportive polymer with a thermochemically responsive one, Leong et al. realized the closing of the microgrippers through the remote trigger of chemicals and temperature under biological conditions.^[35] The aforementioned microgrippers are incompatible with living organisms because of the use of chemicals and metals. To utilize microgrippers in a biocompatible manner, Gracias et al.^[36] developed a methodology for activating the closing of microgrippers via enzymes. The sequential degradation of two biopolymers under the respective enzymes realizes the closing and opening of microgrippers. Through this operation, an object can be remotely picked and placed at the desired location. However, the metallic microgrippers can only grasp once due to the lack of ability to reclose and reopen.

Irreversible grasping is insufficient to fulfill the demand of complex manipulation in vivo, and the production of disposable microgrippers is deemed to be a profligate method. Furthermore, biocompatibility and biodegradability are important considerations for robotic surgery. Researchers have dedicated their efforts to developing biocompatible microgrippers with the capability of repeatable grasping. With thermal-responsive hydrogels as the material of the main body, Fusco et al. fabricated untethered and self-folding microrobot platforms via photolithography.^[37] The microrobot platform consists of a group of magnetic alginate microbeads and a near-infrared (NIR) light-responsive hydrogel bilayer structure. The hydrogel bilayer acts as a closed microgripper to grasp magnetic alginate microbeads after releasing the residual stress. The thermally triggered characteristic of hydrogel allows the microgripper to open and release the microbeads over 40 °C. Compared to the metallic microgrippers, the hydrogel microgrippers cannot pick up objects due to their claws with low stiffness.^[38] By embedding a stiff segmented polymer (polypropylene fumarate) in the soft hydrogel, Breger et al.^[39] proposed a polymeric microgripper with the gripping ability and biodegradability. When triggered by heat, the microgrippers can fold completely and present strong stiffness to excise cells. They have the ability of repeatable grasping in response to temperature change. Despite the fact that microgrippers have achieved the grasping ability of human hands, their mobility is limited to magnetic force attraction, thereby constraining their remote pick-and-place capability. To enhance the motility of soft

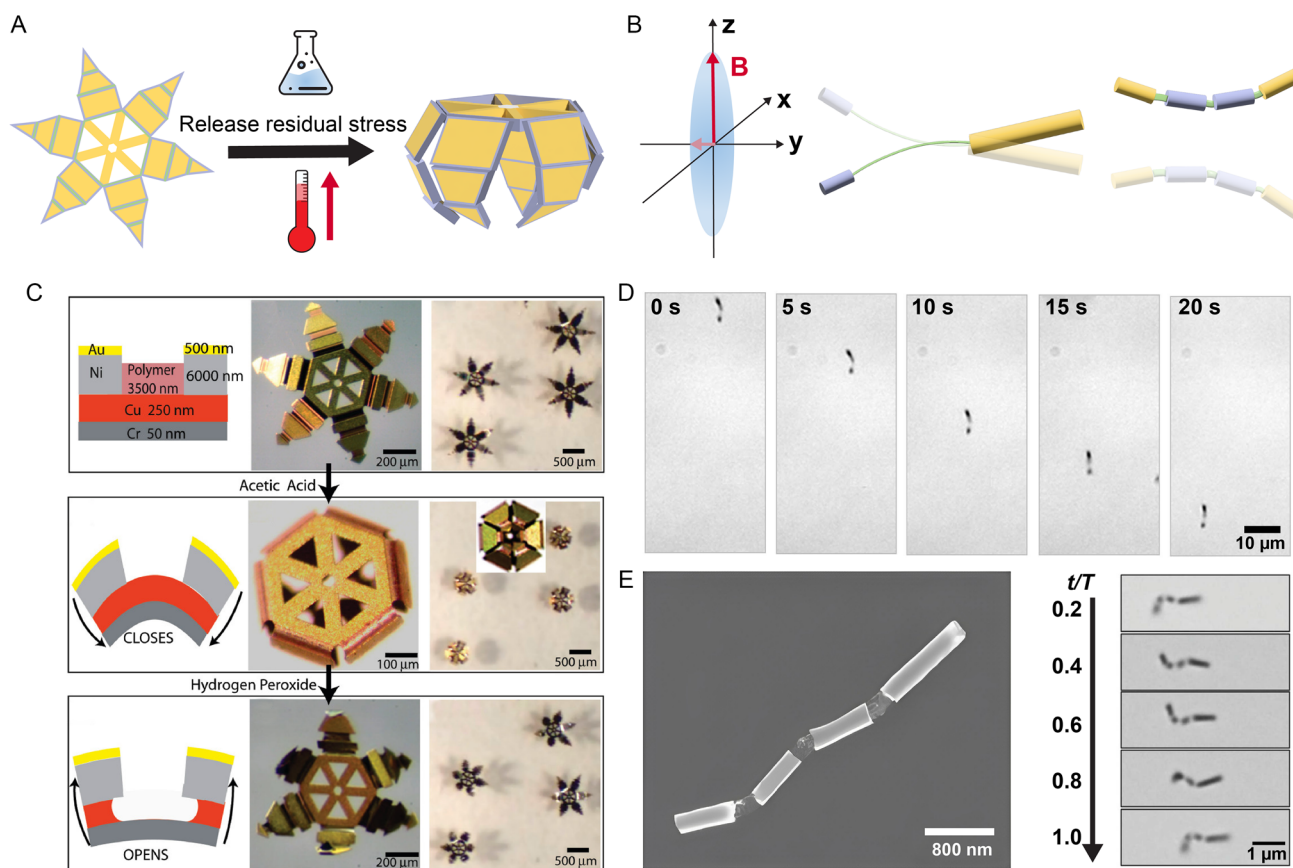


Figure 2. Microrobots with joint or soft segments. A) Schematics of the chemically and thermally triggered closing of a microgripper. B) Rotating motions of segmented microrobots under a rotating magnetic field. C) Schematic diagrams and optical microscopy images of the microgripper with a trilayer joint, including the release, opening, and closing of the microgripper. Reproduced with permission.^[34] Copyright 2008, American Chemical Society. D) Time lapse images of the three-segment microrobots' motion in a urine sample under the rotating magnetic field. The three-segment microrobot is fabricated through the sequential electrodeposition of gold, silver, and nickel. Reproduced with permission.^[22] Copyright 2010, American Chemical Society. E) scanning electron microscopy (SEM) image of the fish-like microrobots and image sequences showing the motion of the microrobot during one cycle by applying an oscillating magnetic field. Reproduced with permission.^[46] Copyright 2016 WILEY-VCH GmbH.

bio-microrobots, researchers are developing microrobots with soft bodies that imitate the flagellar motion of microorganisms or cells.

2.1.2. Microrobots with Soft Segments

By mimicking the flagellar motion, microrobots with soft segments can alleviate the issue of the motility deficiency experienced by microgrippers when executing biomedical tasks. To enable the deformation during movement, soft metallic or polymeric segments are incorporated into microrobots.^[40] The presence of soft segments allows segmented microrobots to bend when subjected to external stimuli. The heterogeneous response of each segment causes time-dependent deformation and consequently enables the microrobots to mimic flagellar beating. The design of segmented microrobots provides an attractive route for replicating the movement of natural microorganisms or cells that are propelled by flagella.

Wang and co-workers used a template electrodeposition method to fabricate bio-microrobots with soft segments. The three-segment microrobots consist of gold, silver, and nickel

segments that are sequentially deposited into the alumina membrane micropores using the electrodeposition.^[22] The length of each segment can be tuned with the deposition time. In the three-segment microstructure, the gold "head" and nickel "tail" are linked by a flexible segment made of a partially dissolved silver part. Figure 2D shows the motion of the three-segment microrobot under a rotating magnetic field. Through the flexible silver segment, the rotating nickel segment drives the gold head to rotate with a different amplitude, thereby breaking the time-reversibility and inducing movement. They have also demonstrated that the forward and backward motion could be achieved by tuning the length of the nickel and gold segments. In contrast to catalytic microrobots that can only work in low ionic-strength conditions, the segmented microrobots break the ionic-strength limitation and display excellent motility. By combining magnetic actuation with catalytic propulsion, Gao et al.^[41] developed soft biomicrobots with hybrid actuation mechanisms. In addition to the previously described three segments, they added a platinum segment at the golden head. The platinum reacts with hydrogen peroxide to generate oxygen

bubbles, which propels the soft microrobots forward.^[42] Under the rotating field without the hydrogen peroxide, the soft micro-robot reverses its swimming direction and moves toward the nickel side. This hybrid actuation manner can enable microrobots to face the situation of fuel depletion and salt limitation. Soft polymeric materials can also be utilized for the fabrication of soft segments in segmented microrobots. Jang et al.^[43] utilized polypyrrole (PPy) to construct the elastic tail of a magnetic three-link microrobot. The elastic tail of the microrobots is connected to two magnetic nickel links via flexible polymer hinges. The hinge's length can be adjusted to change the magnetic dipolar interaction between several nickel links as well as the flexibility of the soft microrobots. The elasticity of PPy allows the three-link microrobot to bend during each stroke, thereby imitating the flagellar beating. Each stroke is generated when the two nickel links respond to the oscillating field. The segmented microrobots with the flagellum-like flexible tail can also be actuated by an acoustic field.^[44] During the actuation excitation, the flexible tail generates propagating waves to propel the head forward as the flagellum of spermatozoa does.

Besides flagellum-inspired microrobots, segmented microrobots can imitate the motion of other creatures. One of the fascinating natural sources is fish species. Most fishes swim with lateral body undulations from head to tail.^[45] Li et al.^[46] reported a magnetic fish-like microrobot composed of four segments (see the image in Figure 2E). To emulate the deformable body of a fish, two gold segments are electrodeposited as the head and the caudal fin, two nickel segments make up the main body, and three flexible porous silver segments connect the gold and nickel segments. Under the oscillating field, the fish-like microrobots bend the magnetic body, causing the entire body to swing, as shown in Figure 2E. The other segmented microrobots include limbed microrobots by linking magnetic Janus microparticles with soft hydrogel structures.^[47] The magnetic Janus microparticles are stabilized with the desired orientation of the easy axis of magnetization through the rigid structures. When exposed to an oscillating field, the magnetic Janus microparticles bend the soft hydrogel after the alignment with the field. The limbed microrobots present lizard-like motion. Inspired by the efficient freestyle strokes for humans, Li et al. proposed a symmetric multisegmented microrobot with two nickel arms, capable of "freestyle" swimming at low Re.^[48] In response to the field, two arms exhibit nonplanar freestyle stroke but with synchronized oscillatory deformations, leading to more efficient swimming ability than existing helical or planar flexible microrobots. However, these microrobots still comprise rigid components that limit their ability to achieve complex deformation, as opposed to those assembled from soft and continuous bodies.

2.1.3. Microrobots with Soft and Continuous Bodies

Microrobots with soft and continuous bodies enable them to adapt to intricate environments within the human body. As male gametes, sperm cells with continuous flagellar deformation are capable of moving to the ovum and achieving fertilization. In the female reproductive tract, they need to travel through the cervix, uterus, utero-tubal junctions, and oviduct before arriving at the ovum.^[16] Soft flagella allow sperm cells to pass through the

utero-tubal junction, a narrow lumen filled with viscous mucus.^[49] The sperm flagellum is a hair-like appendage deformed by the shear and bending forces generated by dynein motors. The deformation of the flagellum results in propagating waves from the head to the tail. The surrounding fluid, in turn, pushes the cell forward, thereby facilitating the movement of sperm cells through narrow passages in the body.

To imitate the flagellum of sperm cells, multiple streptavidin magnetic particles have been linked by biotin double-stranded DNAs to form a long and flexible chain,^[50] as displayed in Figure 3A. The DNA linkers and magnetic particles provide the flexibility and magnetic dipole of the filament, respectively. Moreover, the filament is attached to a red blood cell to constitute a sperm-like microrobot. Under the oscillating field, the filament generates the propagating waves after the alignment of magnetic particles with the external field. This is the first instance of microscopic microrobots emulating the sperm's motion. Apart from the magnetic actuation method, Williams et al.^[51] used cardiomyocytes to actuate the polydimethylsiloxane (PDMS) filament. In Figure 3B, the filament with a short, rigid head and a long but slender tail is fabricated by filling a sperm-shaped channel in a silicon wafer with liquid PDMS, which is followed by the selective culture of cardiomyocytes on the tail. The contraction of cardiomyocytes deforms the soft tail to produce the propagating waves, thereby inducing propulsive thrust to propel the microrobots. Besides, Figure 3C exhibits MagnetoSperms with a magnetic head and a flexible tail through photolithography and physical vapor deposition.^[52] This sperm-like microrobot can be actuated under an oscillating weak field. The magnetization of the magnetic head aligns along the external field and undulates the flexible tail to generate movement. The sperm-inspired microrobots fabricated via photolithography can also be actuated by acoustic field.^[53,54] The artificial flagellum is driven to oscillate and generate the propagating waves when it responds to acoustic streaming. Khalil et al.^[55] and Liu et al.^[56] fabricated magnetic sperm-shaped microrobots via electrospinning, as shown in Figure 3D. During the fabrication process, the polymer solution, including the flexible polymeric material (polystyrene or polycaprolactone), solvent, and magnetic particles, is ejected from a needle with a blunt tip. On account of the electrostatic repulsion among the surface charges, the jet formed at the needle tip deforms into a Taylor cone.^[57] As the jet is stretched into a slender filament, it solidifies quickly under a high voltage and finally deposits on the grounded collector. Bead formation during electrospinning can be attributed to a lot of factors and should be avoided in most applications. For sperm-inspired microrobots, researchers favor the formation of beads that serve as sperm heads. Overall, biologically inspired microrobots have demonstrated exceptional swimming performance. Biohybrid microrobots take it a step further by incorporating living organisms to achieve enhanced motility and functionality.

2.2. Biohybrid Microrobots

Biohybrid microrobots consist of motile microorganisms or cells and functional components. Spermatozoa, bacteria, and algae are widely used to power biohybrid microrobots due to their exceptional motility. Their counterparts, such as polymeric/inorganic

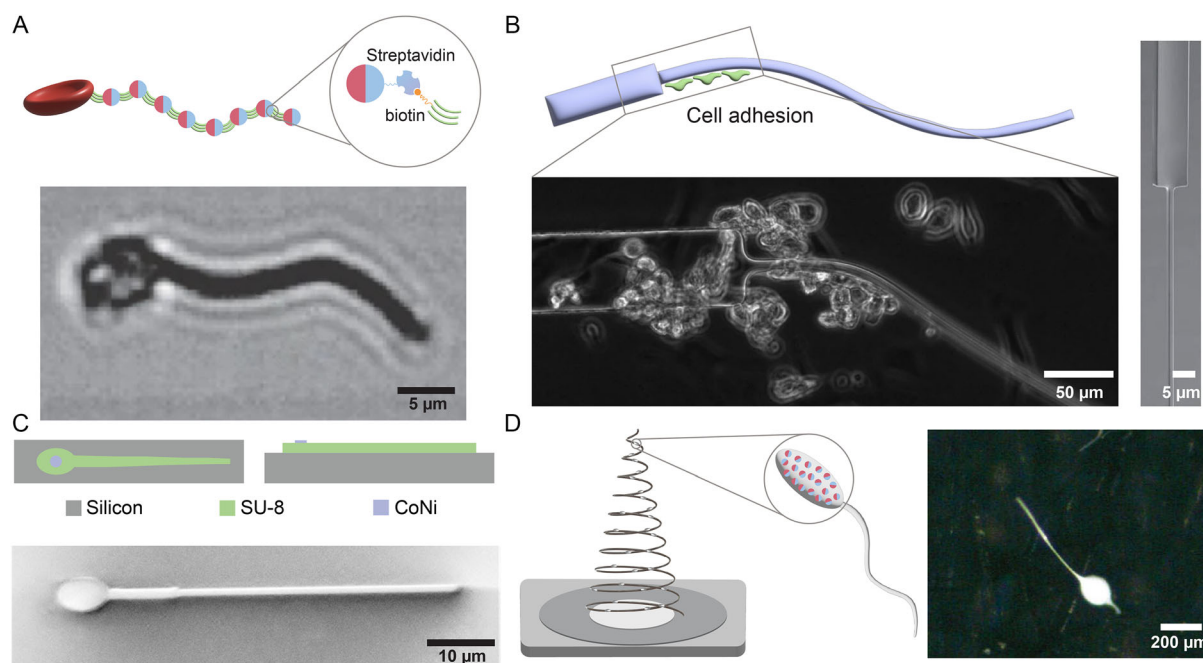


Figure 3. Microrobots with soft and continuous bodies. (A) A chain of magnetic particles linked by DNA is attached to a red blood cell to form a sperm-like microrobot. Reproduced with permission.^[50] Copyright 2005, Springer Nature. (B) The PDMS filament with a rigid head and a compliant tail is actuated by a small, single cluster of contractile cells generating a force through their contraction. Reproduced with permission.^[51] Copyright 2014, Springer Nature. (C) Schematic illustration of the fabrication of MagnetoSperm, and its SEM image. Reproduced with permission.^[52] Copyright 2014, AIP Publishing. (D) Schematic illustration of the fabrication of a sperm-like microrobot through electrospinning, and the optical microscopy image of the electrospun sperm-like microrobot. Reproduced with permission.^[55] Copyright 2016, AIP Publishing.

tubes, micro-/nanoparticles, red blood cells (RBCs), and nanoliposomes (NLs) can endow biohybrid microrobots with additional capability, including magnetic steerability, drug loading and release, and interaction with targeted cells. The functional components can be integrated with motile microorganisms or cells through physical binding or chemical bonding, as shown in **Figure 4**. For example, the magnetic microtube can trap and transport microorganisms along the magnetic field. However, this physical binding approach may be unstable. The integration of chemical bonding in biohybrid microrobots offers a stable connection between microorganisms or cells and functional components and allows the release of microorganisms or cells under external stimuli. According to the category of microorganisms or cells, biohybrid microrobots encompass sperm-based microrobots, bacteria-driven microrobots, and algal microrobots.

2.2.1. Sperm-Based Microrobots

Through the coordinated cooperation of dynein motors, including their attachment and detachment from the flagellar microtubule, the sliding of the microtubule is transformed into the bending motion of the flagellum,^[58] which ultimately leads to sperm cells' swimming. Alive sperm cells can be attached to artificial components to realize directional control, biomedical tasks, and visualization. Sperm-bots,^[27] which consist of a sperm cell and an artificial magnetic microtube (see **Figure 5A**), is the first example of sperm-actuated microrobots. The magnetic cap is created through the rolled-up technology^[59] and randomly captures

alive sperm cells. The incorporation of an iron layer in the cap enables live sperm cells to realize directional control under a magnetic field. A point-to-point closed-loop control has been implemented to precisely control the sperm-bots using four electromagnetic coils and visual feedback through a microscopic camera system.^[60] A thermally responsive polymer has been utilized to enable a remote release mechanism for the sperm cell.^[61] After the temperature is elevated by a few degrees, the tubular cap unfolds and releases the captured sperm cell. The remote-controlled capture and release without damage to sperm cells are significant for assisted fertilization. To realize spatially and temporally controlled release, a magnetically driven microcarrier and a synthesized protein-based hyaluronic acid (HA) microflake have been employed to transport and capture sperm cells, respectively.^[62] A helical microcarrier is fabricated by two-photon polymerization lithography and coating with a thin iron film. This microhelix transports the sperm-loaded microflakes consisting of HA. Sperm cells can bind to HA microflakes through their innate HA receptors.^[63] Upon reaching the targeted location under magnetic guidance, the HA microflake undergoes enzymatic hydrolysis, leading to the release of sperm cells from the microcarrier. The ultimate goal of sperm-driven microrobots is to aid in fertilization as sperm cells are the reproductive cell in males.^[64] As a method to trigger single sperm maturation and protection from oxidative stress with the help of artificial microstructures, Ridzweski et al. used gelatin sperm-bots for the pH-triggered release of heparin.^[65] The gelatin-based sperm-bots also allowed the successful degradation of microrobots. To

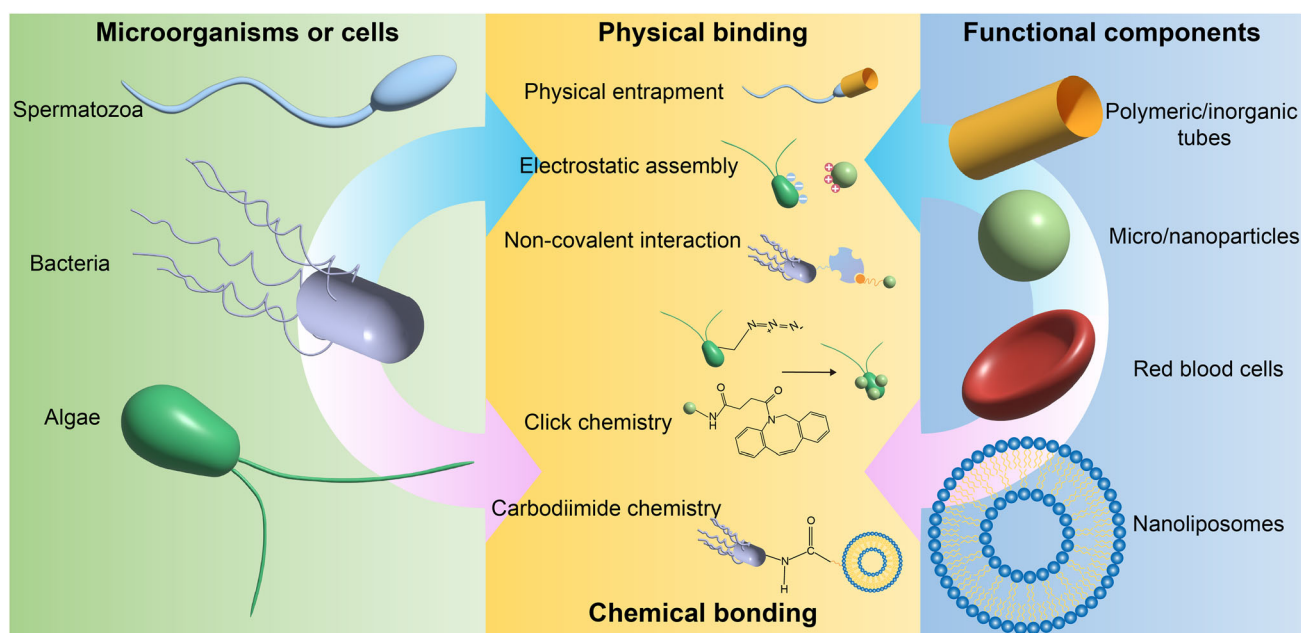


Figure 4. Biohybrid microrobots comprise motile microorganisms or cells and functional components. Microorganisms or cells such as bacteria, algae, and spermatozoa can be combined with functional components including polymeric or inorganic tubes, micro/nanoparticles, red blood cells, and nanoliposomes through physical binding or chemical bonding. These functional components can endow microrobots with the ability to complete biomedical tasks, steer, and visualize.

address the problems of low sperm count, also called oligospermia, Rajabasadi et al.^[66] developed a 4D-printed multifunctional microcarrier to transport and deliver multiple sperm cells. The captured sperm cells are capitulated in situ after contacting the loaded heparin in the microcarrier. The hyaluronidase-loaded polymersomes functionalized on the microcarrier's surface can facilitate the degradation of cumulus cells, addressing the issue of infertility due to the lack of hyaluronidase. Even though the incorporation of a magnetic microcarrier enables the directional control of sperm cells, the sperm cells reduce their speed when they are captured by the artificial microcap or microcarrier. Motile sea urchin sperm have also been used in combination with magnetic nanoparticles to create chemotactic sperm microrobots for active drug delivery.^[67] As much as spermbots are beneficial due to their onboard power source, their lifetime is limited to a few hours which makes their fabrication and implementation for in vivo applications challenging.

Another typical sperm-based microrobot is a type of sperm-templated microrobot. Figure 5B shows the biotemplated IRONSperm, which comprises nonmotile sperm cells and rice grain-shaped magnetic nanoparticles via the electrostatic self-assembling.^[68] Sperm cells are not alive after binding to magnetic nanoparticles, as opposed to spermbots. Therefore, IRONSperm does not undulate its flagellum through the coordination of dynein motors. The power of IRONSperm is provided by an external field, guaranteeing its long-term motility. In the presence of the field, the passive flagellum will bend under the alignment of magnetic nanoparticles with the external field and generate propagating waves to propel the cell body. Khalil et al.^[69] demonstrated that IRONSperms with the passive flagellum can exhibit waveforms to match that of motile cells

by adjusting the external field. With the template of the biological entity, chemotherapeutic agents can be absorbed.^[68] The biocompatibility of IRONSperms sets it apart from sperm-inspired microrobots made entirely of synthetic materials and shows its huge prospects for biomedical applications. IRONSperm clusters can be formed under the influence of magnetic attraction and electrostatic self-assembly.^[70] Compared to one single IRONSperm, the cluster can highly increase the drug loading capability and be localized using ultrasound imaging for in vivo applications. Although IRONSperm has shown promise for targeted drug delivery, it still needs further development for efficient and controlled drug loading and release at the target sites.

2.2.2. Bacteria-Driven Microrobots

Bacteria-driven microrobots stand out from various types of biohybrid microrobots, considering their efficient propulsion speed, interaction ability, and sensing capability in physiological and pathophysiological conditions.^[71] Some bacteria have demonstrated that they can adhere well to a polymeric or metal layer due to their charged and hydrophobic cell membrane. By combining bacteria with polymeric particles, polymer tubes, RBCs, NLs, or nanoparticles, bacteria-driven microrobots can be bestowed with additional functionalities, such as magnetic maneuverability, drug encapsulation and release, and fluorescence. The common bacteria used in the development of bacteria-driven include *Serratia marcescens* (*S. marcescens*), *Escherichia coli* (*E. coli*), and *Magnetococcus marinus*. *S. marcescens* is a specie of Gram-negative bacterium with appendages of helical flagella. The rotation of these flagella is powered by a rotary motor embedded in the bacterial cell wall.^[72] The peculiar helical

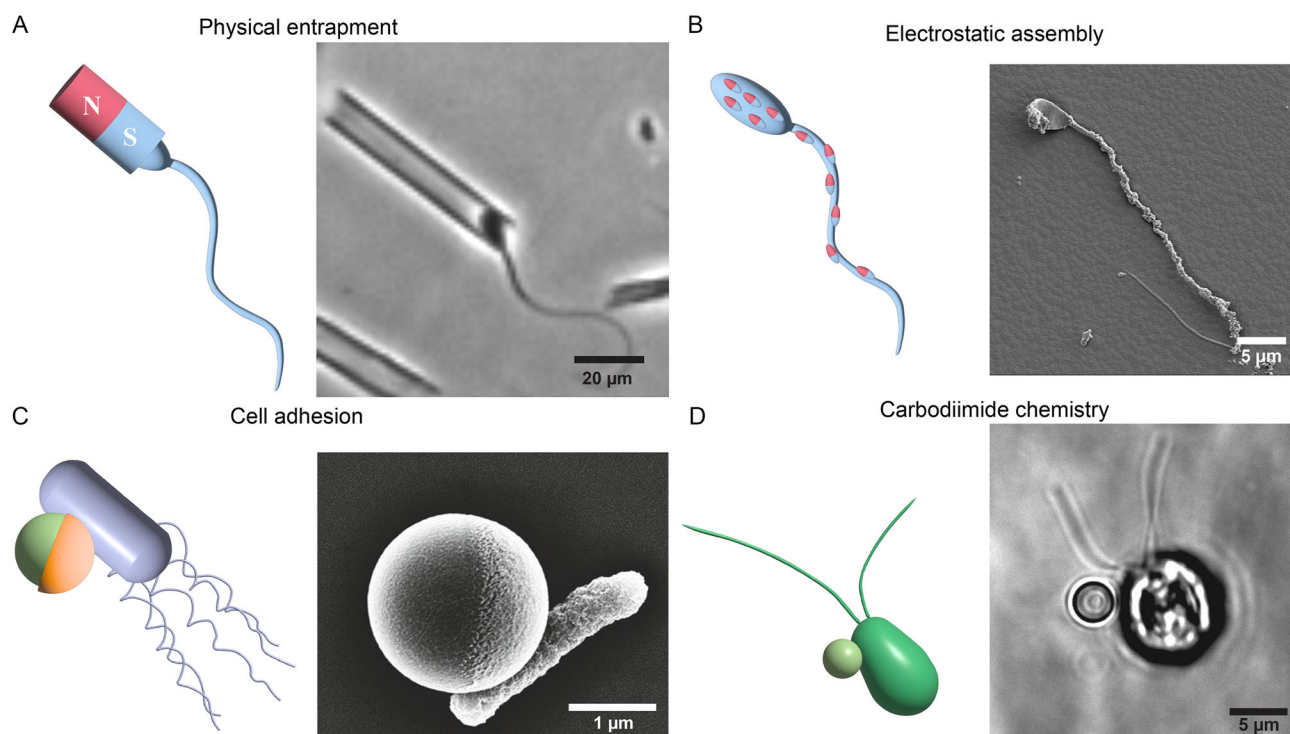


Figure 5. The biohybrid microrobots using spermatozoa, bacteria, or algae. A) Optical image of a spermbot, which consists of a sperm cell and a magnetic microcap. B) IRONSperm: the cryoscanning electron micrograph shows a bovine sperm cell covered with iron oxide particles through the electrostatic assembly. C) SEM image of the bacterium *E. coli* attached to the Janus particle. Reproduced with permission.^[78] Copyright 2015 WILEY-VCH GmbH. D) Optical microscopy image of a bead attached to the alga *C. reinhardtii*. Reproduced with permission.^[88] Copyright 2005, National Academy of Science, U.S.A.

structure can break the time reversibility in the low-Re regime. However, the motion of *S. marcescens* is subjected to stochastic direction changes, which impedes their precise control. To address this problem, *S. marcescens* have been attached to magnetic beads through streptavidin–biotin binding.^[73] The bacteria provide the power of motility, while the magnetic beads offer the magnetic dipole to realize the steering control of the bacteria under the magnetic field. They have demonstrated the controlled steering of the microrobots driven by *S. marcescens*. The dimension of these microrobots is smaller than sperm-like microrobots, thereby allowing them to navigate in tiny passages. Moreover, Zhuang et al. demonstrated that the microrobots driven by *S. marcescens* exhibit both unidirectional and bidirectional pH-tactic behaviors in the configured pH gradients.^[74] *S. marcescens* can stop and resume their motion after being triggered by chemical signals^[28,75] and ultraviolet light.^[76] The pH-tactic, chemotactic, phototactic, and magnetic control can be combined for the motion control of microrobots driven by *S. marcescens* in the future.

Not all bacteria can adapt to the human body temperature, certain bacteria's motility is sensitive to temperature. Nonpathogenic *E. coli*, which are commonly found in the lower gastrointestinal (GI) tract, can maintain or even increase their swimming speed at 37 °C. *E. coli* is one type of peritrichously flagellated bacterium that propels itself through the rotation of helical flagella. During the “run” motion, all flagella rotate counterclockwise and form a bundle. In this case, *E. coli* move in a straight path. At the “tumbling” motion, one or more flagellar

motors reverse their rotation. As a result, the flagella unbundle, enabling the bacterium to change its orientation.^[77] *E. coli* are promising entities for the fabrication and actuation of soft bio-microrobots due to their motility and adaptability. The ability of *E. coli* to adhere to a variety of metals, such as platinum, iron, titanium, and gold, has been demonstrated. Stanton and co-workers have reported a biohybrid Janus robot by attaching *E. coli* to polystyrene particles or silicon dioxide covered with a metal layer,^[78] as shown in Figure 5C. These bacteria-driver microrobots show the ability to deliver the particles along the magnetic field when the iron is coated on the particles. They have also fabricated electropolymerized microtubes to trap *E. coli*.^[79] The polydopamine-modified microtube is positively charged and acts as a surface attractant for the negatively charged *E. coli*. Besides, the layer of nickel nanoparticles for magnetic guidance and urease to act as a bacterium “killer” are included in the microtube. The urease decomposes urea and creates a local distribution of ammonia to inhibit the bacterium swimming. Compared with the spherical chassis, the microtubular chassis can reduce the rotating motion and the torque when attaching to the bacteria. RBCs are excellent companions for bacteria due to their abundance, biocompatibility, biodegradability, non-immunogenicity, inert intracellular environment, and handling convenience. Alapan et al.^[80] reported a biohybrid microrobot composed of motile *E. coli* and RBCs loaded with an anticancer drug and iron oxide nanoparticles for actively guided drug delivery. The onboard power is provided by the bacteria, while

the magnetic guidance is realized through the loaded magnetic nanoparticles. On-demand hyperthermia activated by the NIR light is realized to terminate the bacteria after drug delivery. A genetically engineered *E. coli*-based biohybrid microrobot has been decorated with magnetic nanoparticles for externally guided magnetic control and pH- and light-responsive NLs for on-demand cargo delivery in tumor spheroids.^[81]

Magnetotactic bacteria (MTB) are motile prokaryotes that are able to biomineralize nanometric magnetic particles, known as magnetosomes.^[82] These magnetosomes are organized as well-ordered chains, allowing bacteria to behave like a compass needle and navigate along the Earth's magnetic field. Moreover, MTB are nonpathogenic and easy to be chemically functionalized. All of these properties make MTB viable candidates for in vivo biomedical applications. *Magnetococcus marinus* strain MC-1 is one type of spherical MTB with two flagella bundles, synchronously pushing the cell forward. Martel and co-workers realized the control of MC-1 through a customized electronic system.^[83] They have also found that the swimming of MC-1 can stop with sufficient field strength. A closed-loop navigation control on the MC-1 is achieved based on the visual feedback from a clinical magnetic resonance imaging system. After that, a swarm of MC-1 bacteria is formed in 2D^[84] and 3D^[85] configurations through a time-varying magnetic field. In addition, bacteria aggregation is suited to undertake tasks in intricate microvascular networks of the human body. The bacterial-driven microrobots swarm can achieve high targeting efficacy and deliver an adequate dose of therapeutics to tumor cells. The other MTB, *Magnetospirillum magnetotacticum* (MS-1), has a helical shape and is propelled by a polar flagellum at each end of the cell. Khalil *et al.* realized a point-to-point control on the movement of MS-1 after understanding the characteristic of its magnetic moment.^[86] A null-space control system is presented to achieve point-to-point control of MS-1 by capitalizing on the redundancy of magnetic-based manipulation systems. When designing bacteria-driven microrobots, the careful evaluation and selection of motile bacteria are crucial. In particular, the selection process should take into account the intended biomedical applications, size, swimming speed, and ability to interact with polymeric materials. Schürle *et al.* demonstrated the magnetic torque-driven enhanced crossing of biological barriers to enter deep tumor tissue by the implementation of liposome-functionalized *Magnetospirillum magneticum*-driven microrobots.^[87]

2.2.3. Algal Microrobots

As eukaryotic swimmers with facile culture processes, microalgae present high speed, phototactic guidance capability, and autofluorescence. For example, *Chlamydomonas reinhardtii* (*C. reinhardtii*) is a unicellular green alga with a spherical-shaped head and two flagella. The full beat cycle of *C. reinhardtii* is composed of a power stroke and a recovery stroke. During the power stroke, each flagellum extends and bends at the proximal end, sweeping back like the breaststroke. The flagellum then folds during the recovery stroke to reduce viscous drag. This strategy is used to break time reversibility. *C. reinhardtii* can perform photosynthesis for oxygen production, which can relieve the hypoxic conditions at the wound site. Due to these characteristics,

C. reinhardtii can be an ideal choice to achieve targeted cargo delivery. Weibel *et al.* utilized *C. reinhardtii* as a "microoxen" to move microbeads.^[88] The microoxen can be steered using the phototaxis of *C. reinhardtii*. Polymeric microbeads are loaded to the microoxen via a photocleavable linker and released photochemically in Figure 5D. *C. reinhardtii* can also be combined with magnetic materials to mimic MTB. Santomauro *et al.* found that *C. reinhardtii* can be magnetized after incorporating terbium.^[89] The modified algae can show comparable magnetic moments as MTBs and be magnetically steered. *Eudorina elegans* (*E. elegans*) is a multicellular green alga specie with a size ranging from 10 to 200 μm . *E. elegans* exists in the form of colonies, which consists of 16, 32, or 64 individual cells with a similar size as *C. reinhardtii*. They display positive phototaxis and swim toward a light source. This property makes it possible to control the movement of *E. elegans* and exploit them in micro-/nanodevices, biological chips, and biomedical applications. Xie *et al.*^[90] built an algae guiding system to steer *E. elegans*. The motion along predefined trajectories such as zigzag and triangle could be realized under optical control with a specific wavelength. The inherent autofluorescence ability of the microalgae enables them to be visualized and tracked in real time. These algal microrobots with biocompatibility and controllability hold great promise for cancer treatments. Akolpoglu *et al.*^[91] have created high-throughput fabrication of *C. reinhardtii*-based microrobots by electrostatic assembly with magnetic nanoparticles. On-demand cancer drug delivery has been demonstrated with these biohybrid microrobots.

3. Energy Sources for Soft Bio-Microrobots

Because of their tiny size, soft bio-microrobots can not use onboard batteries to power themselves as macrobots do. Existing soft bio-microrobots move by converting the power of the external field to their kinetic power or using the self-propulsion of microorganisms or cells. The common external fields include magnetic, optical, and acoustic fields. The incorporation of the external field could be a stimulus to deform the body of soft bio-microrobots for movement or manipulation. In addition, by consuming molecules that contain chemical energy, microorganisms or cells achieve inherent mobility, which is utilized in the self-propulsion approach. Upon the modification with externally responsive materials, live microorganisms and cells can be transformed into maneuverable microrobots when subjected to external fields. In the next sections, we give a comprehensive explanation in terms of energy sources used by soft bio-microrobots.

3.1. Magnetic Actuation

Magnetic actuation is a practical choice for controlling microrobots in minimally invasive medicine because of its high penetration capability and safety with biological samples.^[92,93] The two types of magnetic actuation are force actuation and torque actuation. In this section, we shall present the fundamental laws that govern the magnetic force and torque exerted on the soft-magnetic bodies of microrobots. Magnetic microrobots experience a magnetic force, F , and a magnetic torque, τ , provided

that a magnetic field is applied. The magnetic force, \mathbf{F} , exerted on the microrobot can be expressed as, $\mathbf{F} = V(\mathbf{M} \cdot \nabla)\mathbf{B}$, where V and \mathbf{M} are the volume and the magnetization of the magnetic material of the microrobot, respectively, and \mathbf{B} is the magnetic flux density of the external magnetic field. The magnetization depends on the external field, as the relationship $\mathbf{M} = \chi_a \mathbf{H}$ holds, where χ_a and \mathbf{H} are the susceptibility tensor of the material and the magnetic field strength, respectively. In a magnetic gradient field, the magnetic microrobot experiences both magnetic torque driving the magnetization to align with the external field and the magnetic force pointing to the direction of increasing strength, as shown in **Figure 6A**. The magnetic force has been utilized for pulling the microrobots,^[94,95] resulting in linear movement of microrobots. Its direction can be tuned with that of the gradient.

In a uniform magnetic field, magnetic torque is the only form of energy transmission to power magnetic microrobots. The magnetic torque, $\boldsymbol{\tau}$, can be given by, $\boldsymbol{\tau} = V\mathbf{M} \times \mathbf{B}$. The magnetic microrobot is magnetized and generates magnetization when subjected to the magnetic field. In the presence of a magnetic torque, the magnetization of the microrobot will align with the direction of the external field. To ensure the continuous movement of microrobots, the magnetic field should vary in time or space. **Figure 6B** exhibits the common magnetic fields used for torque actuation, including rotating field,^[96,97] conical rotating field,^[68] and oscillating field.^[52,98] The rotating field is characterized by a field vector that rotates in a plane, frequently at a constant angular velocity. On the other hand, the conical rotating field refers to an out-of-plane field that follows a cone, which is typically produced by a rotating field vector and a static field vector perpendicular to it. Finally, the oscillating field is defined by a field vector moving up and down in the plane and is commonly used to produce flagellar motion in soft bio-microrobots.^[99] Although the magnetic field has been proven to be an effective energy source in wireless actuation, other energy sources can be used individually or in combination to enhance the capability of the microrobots.

3.2. Acoustic Actuation

Since ultrasound technology has been widely used in medical diagnosis and therapeutics, researchers have focused on the development of microrobots powered by an acoustic field. The acoustic field can be exploited in the forms of acoustic radiation force and acoustic streaming.^[100] When a standing wave is applied to a resonator, it reflects back and forth and creates a hydrodynamic drag force, known as the acoustic radiation force, F_{rad} , in a fluid for driving microrobots to the acoustic pressure nodes and antinodes, as shown in **Figure 6C–i**. The direction of force can be changed with the corresponding wave function.^[101] The magnitude of the acoustic radiation force is given by, $F_{\text{rad}} = 2\alpha I/c$, where α is the absorption coefficient of the medium, I is the temporally averaged intensity at the spatial location, and c is the sound speed.^[102] The radiation forces include the primary and secondary radiation forces. The primary radiation forces are generated due to the interaction between the acoustic field and the microrobots in the medium. The reflected wave from the microrobot can induce the secondary radiation forces on an adjacent microrobot.^[12] The primary radiation force

propels microrobots to the nodal position, while the secondary radiation forces make microrobots mutually attract or repel and generate a stable microrobot swarm.^[103] However, the standing wave cannot be established in the human body in a predictable manner, as complex and heterogeneous environments can affect the formation of standing waves. For example, the presence of internal organs, bones, and tissues with different mechanical properties can scatter and absorb the acoustic wave. Therefore, the acoustic force is a challenging actuation method for in vivo biomedical applications of microrobots.

Acoustic streaming is a steady fluid flow formed by viscous attenuation of an acoustic wave.^[104] Due to the excitation of the acoustic streaming, the flagellum-like segmented microrobots produce propagating waves (see **Figure 6C–ii**), thereby propelling themselves forward. Soft bio-microrobots can be fabricated in situ and actuated by acoustic streaming. In the presence of the streaming effect, the flagellum of the soft microrobot oscillates and generates propulsive thrust.^[54] Acoustic streaming can also be enhanced with solid boundaries such as a sharp extrusion^[53,105] or the “horse-shoe” structure.^[106] The vibration of these structures induces counterflowing vortices in the near field that results in a steady flow in the far field, thus generating controllable acoustic waves. Although the acoustic actuation method has been extensively used in soft microrobots, it still faces the challenge of directional control of soft bio-microrobots. The precision of motion control influences the in vivo application prospects of soft bio-microrobots.

3.3. Optical Actuation

The optical actuation can be exploited in synthetic microrobots and phototaxis microorganisms. In terms of synthetic microrobots, light-responsive materials are implemented to constitute the main body of the microrobots. The optically actuated microrobots rely on the deformation of body parts to achieve movement.^[107] The most used light-responsive material is liquid-crystalline elastomers (LCEs) that can deform when exposed to light. LCEs possess the entropy elasticity of an elastomer and the self-organization of the liquid crystalline phase. Their entropy elasticity enables them to stretch and bend, while the self-organizing characteristic provides the ability to respond to external stimuli and adjust their structure. There are two main mechanisms for the shape deformation of light-responsive materials. The first one is the shape change of part of the molecule after exposure to light, and the second one utilizes intermediate heating induced by light absorption to change a shape. The photothermal effect can result in an order–disorder phase transition in LCEs,^[108] as shown in **Figure 6D–i**. Palagi et al.^[7] have shown that soft microrobot can mimic the metachronal waves of ciliated protozoa. The biomimetic motion is achieved by incorporating photoactive LCEs and controlling their shape through spatially and temporally modulated monochromatic light. The LCEs deform upon illumination based on the principle of the photoisomerization of the covalently bound azobenzene dye and a light-induced thermal effect.

Some microalgae possess positive (swim toward the light source) or negative (swim away from the light source) phototaxis when triggered by an external light source. For example,

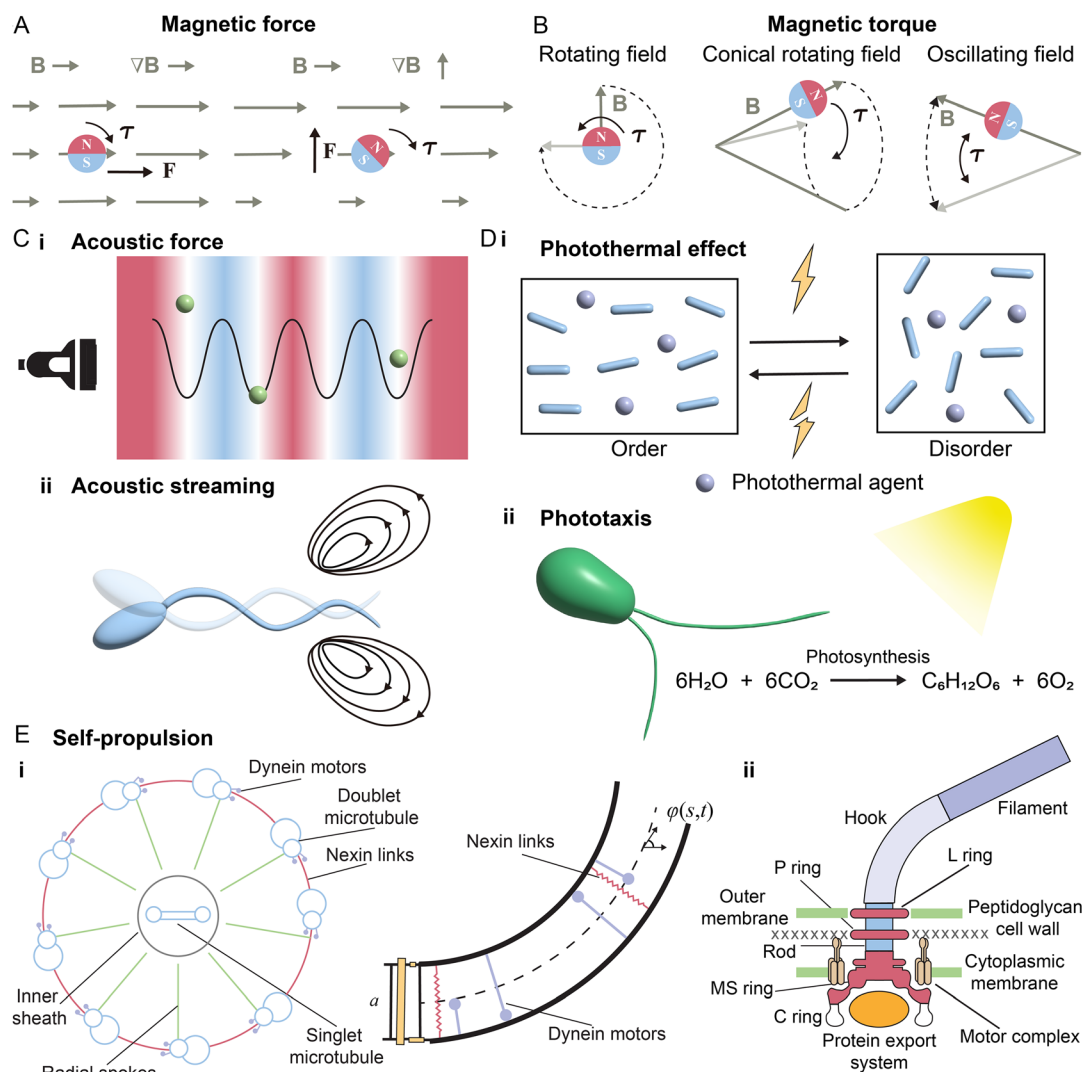


Figure 6. Actuation mechanisms of soft bio-microrobots. (A) Magnetic force actuation. The magnetic force is generated by the field gradient along the direction of the field and the field gradient perpendicular to the direction of the field. (B) Magnetic torque actuation. The magnetic torque is generated by the rotating field vector in a plane, the rotating field along the mantle of a cone, and an oscillating field in a plane. (C) Schematics of acoustically actuated mechanisms. (i) Acoustic radiation force acts on spherical microrobots, which aggregate at the acoustic pressure nodes and antinodes. (ii) Schematic of acoustic streaming at the tip of a sperm-like microrobot. The acoustic streaming generated by the deformation of the flagellum propels the microrobot forward. (D) The mechanism of optical actuation. (i) LCEs deform after photothermal-induced order–disorder phase transition triggered by lights. (ii) Phototaxis of microalgae is triggered by their photosynthesis. (E) Chemically powered self-propulsion of microorganisms or cells. (i) Schematics of the cross section of the eukaryotic flagellar axoneme. The flagellum is bent by the shear force, which is produced by the attachment and detachment of dynein motors. (ii) Schematic side view of the H^+ or Na^+ bacterial flagellar motor. The motor, spanning the outer membrane, peptidoglycan cell wall, and cytoplasmic membrane, has a series of hinges with a rod inside. Attached to the rod is a curved ‘hook’ protein linked to the flagellum. The flagellum is made of thousands of repeating units of the protein flagellin.

C. reinhardtii exhibits the positive phototaxis to increase photosynthesis, yet it also swims away from light to avoid damage to molecular complexes used in photosynthesis.^[109] The photoreceptors on cell membranes can detect the direction of illumination, and enable cells to find an appropriate condition to complete photosynthesis (see Figure 6D-ii). The nutrition produced during photosynthesis provides the energy for locomotion. The second requirement for phototaxis is motility, which is provided by the flagella of microorganisms or cells. We will elaborate

on the locomotion mechanisms of microorganisms and cells in the next section.

3.4. Self-Propulsion

Microorganisms and cells are able to move owing to their sophisticated appendages, known as flagella. The soft flagella generate bending waves through self-organization and powering of their

internal molecular motors. After interacting with the surrounding fluid, the deformable flagella will induce propulsive thrust. Therefore, motile microorganisms and cells can serve as viable candidates for microrobots used for biomedical applications. The generic flagellated microorganisms and cells include spermatozoa,^[110] flagellated bacteria,^[111,112] and algae.^[15] To understand the locomotion mechanism of eukaryotic flagella (sperm cells and algae), the flagellar structure should first be clarified. Figure 6E-i shows the illustration of the flagellar axoneme, which is known as the “9 + 2” structure.^[16] Nine pairs of microtubule doublets and a central pair of singlet microtubules comprise the flagellar axoneme. The adjacent microtubule doublets are connected by nexin links, while radial links bind the central pair of single microtubules to the surrounding microtubule doublets. Dynein motors are distributed along the nine pairs of microtubule doublets. They undergo cycles of attachment and detachment to generate shear force with the force density, f , by hydrolyzing the adenosine triphosphate, thus causing the sliding between the microtubule doublets and bending of the flagellum. The flagellum oscillates in a time-periodic manner such that the elastic force and the bending force are balanced by the viscous force. The tangent angle, $\varphi(s, t)$, is used to characterize the flagellar deformation of a flagellum, as shown in Figure 6E-i. The flagellum elastohydrodynamics are given by the balance of the elastic force per meter square, $-E\varphi_{ss}$, the internal bending force per meter square, $a\varphi_t$, and the viscous force per meter square, $\xi_1\varphi_t$, where E is the bending stiffness of the flagellum, the subscript s and t denote spatial derivative and temporal derivative, respectively, and a and ξ_1 are the constants of the two polar filaments and the normal drag coefficient of the flagellum, respectively.^[113] This nonlinear differential equation can assist in analyzing the deformation of the flagellum during the movement. The solved position of the flagellum can be implemented into other theories, such as resistive force theory,^[110] and regularized Stokeslets theory,^[114] to characterize its propulsion ability. The excellent motility and deformability allow spermatozoa and algae to swim in the compact space of the human body. Prokaryotic (bacterial) flagella are fundamentally different from eukaryotic flagella in that the thrust of the tail is generated at the base of the tail. It consists of a rotary enzymatic motor which is embedded in the bacterial membrane and is fueled by H^+ or Na^+ transport driven by an electrochemical gradient,^[115] as shown in Figure 6E-ii. The bacterial flagella follow this rotation passively, which is in contrast to the bending wave motion of spermatozoa with active molecular motors all along the tail.

4. Biomedical Applications of Soft Bio-Microrobots

The above sections discuss the design principles and energy sources of soft bio-microrobots, forming the basis for their use in biomedical applications. The flexible structure of soft bio-microrobots allows them to navigate through narrow blood vessels or bend around tight corners within the human body. Furthermore, the soft composition of their bodies can reduce the risk of scratching healthy tissue or cells when performing biomedical tasks *in vivo*. These advantages make soft bio-microrobots highly effective and versatile tools for

biomedical applications. In this section, we will introduce the related biomedical applications of soft bio-microrobots, including targeted delivery and surgery.

4.1. Targeted Delivery

Because cancer treatment still relies on the circulatory system of the human body to deliver anticancer drugs, the efficacy of reaching the cancer lesions is extremely low through this passive manner.^[116] Meanwhile, a drug that is not targeted specifically to tumor cells can cause side effects on healthy cells and organs. An active delivery system using the proposed microrobots can increase the accumulation of drugs in the cancer lesions, as well as reduce the risk of side effects. Therefore, microrobots capable of precise control and cargo loading are suitable medical tools for actively targeted cargo delivery. The delivered cargo can be drugs, micro-/nanoparticles, and living cells. Untethered microgrippers can be steered using a magnet and use the stiff phalanges to pick up beads after the gripper closure is triggered by chemicals and temperature.^[35] Figure 7A shows the thermally triggered capture of a dyed bead from several clear beads. The beads inside the grippers can be released intact by mechanical disruption. Unlike microgrippers, segmented microrobots can load cargo through physical and chemical binding. Gao et al. reported the targeted delivery of drug-loaded magnetic polymeric particles utilizing segmented microrobots.^[117] The drug-loaded magnetic microparticles can be magnetically attracted by the nickel segment when the segmented microrobots pass close by them under the magnetic field. After reaching the HeLa cells, the flexible silver segment of the microrobots is bound to the cell and enables the slow release of drugs from the microparticles, as shown in Figure 7B.

Compared with synthetic soft microrobots, sperm cells are more advantageous to operate in physiological environments due to their nontoxic qualities. Xu et al. proposed an efficient drug delivery system using spermatozoa,^[118] as sketched in Figure 7C. The spermatozoa carries an anticancer drug, doxorubicin hydrochloride (DOX-HCL), through physical encapsulation. This drug delivery system has high drug-carrying stability during the delivery process due to the compact membrane of sperm cells. The magnetic cap is designed to have a tetrapod microstructure and releases the captured sperm cells when it hits a substantial barrier. This capability is exploited to liberate the drug-carrying sperm cells in the scenario when the spermatozoa strike the cancer spheroid. To increase successful cargo load, Xu et al.^[119] fabricated a spermatozoa system that transports up to three human sperm cells using a streamlined microcap. The spermatozoa system can carry a hydrophilic drug, DOX-HCL, via uptake by sperm cells, and a hydrophobic drug, camptothecin, on the microcap for the treatment of cervical cancer and ovarian cancer. This method of codrug administration opens new doors for future targeted drug delivery. The biotemplated IRONSperms have loaded DOX-HCL for therapeutic tasks.^[68] DOX-HCL molecules can be absorbed and distributed in the whole body of IRONSperms through physical encapsulation. The tight sperm membrane ensures the stability of drug encapsulation and avoids drug leakage during the movement.

Proliferative tumor cells can rapidly consume oxygen, thereby resulting in a hypoxic region with less oxygen compared to

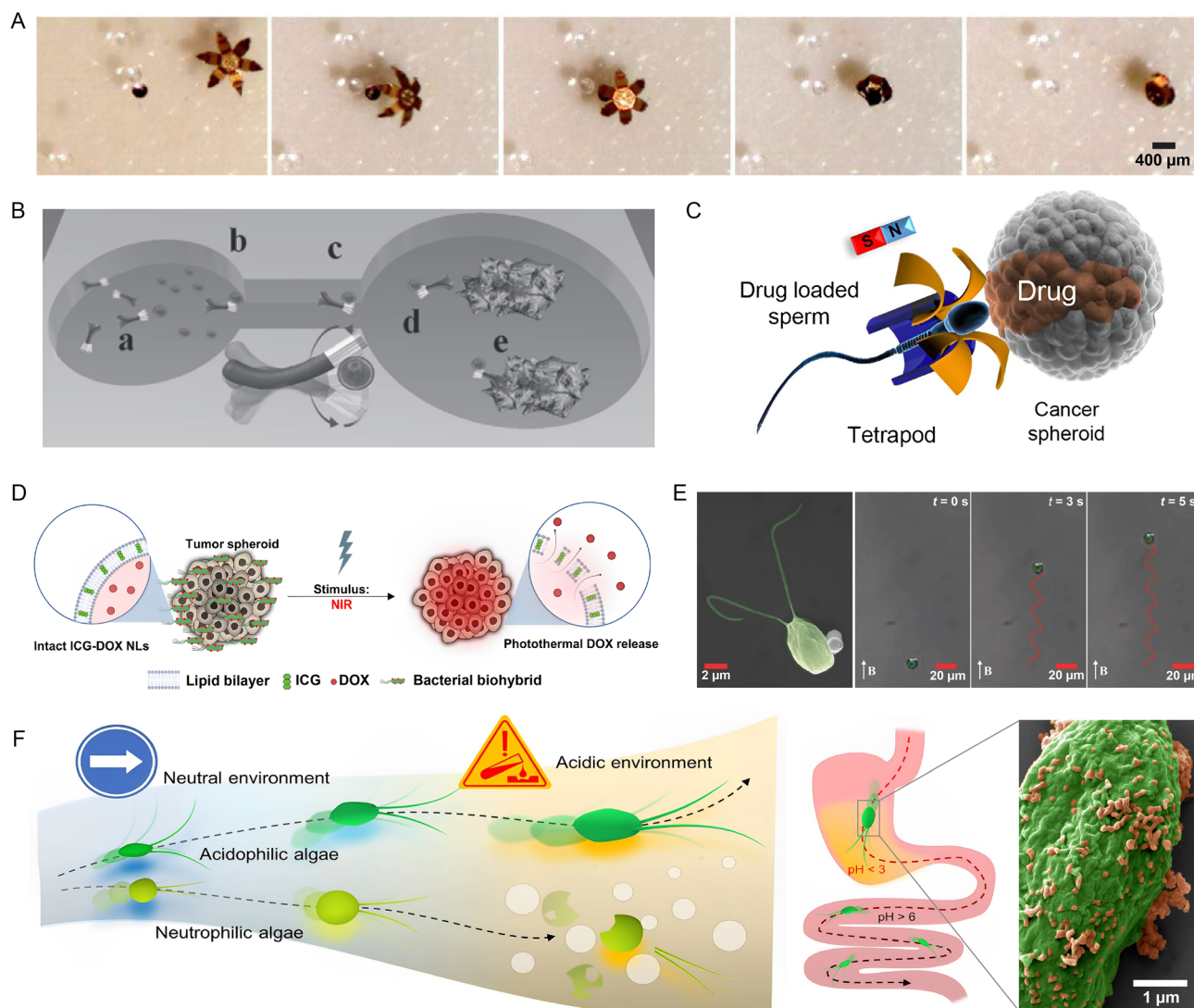


Figure 7. Targeted delivery applications of soft bio-microrobots. A) Optical microscopy image sequence showing the thermally triggered capture of a dyed bead from several clear beads. Reproduced with permission.^[35] Copyright 2009, National Academy of Science, U.S.A. B) Schematic depicting the process as a segmented microrobot a) captures the drug-loaded magnetic polymeric particles in the loading reservoir, b) transports it through the channel, c) approaches the targeted cell, d) sticks on the targeted cells, and e) releases the drug. Reproduced with permission.^[117] Copyright 2012, WILEY-VCH GmbH. C) Schematic of a drug-loaded spermbot targeted delivering to a cancer spheroid. Reproduced with permission.^[118] Copyright 2017, American Chemical Society. D) Bacteria-driven microrobots carrying stimuli-responsive ICG-DOX NLS are localized on tumor spheroids and release their payload upon NIR stimulus. Reproduced with permission.^[81] Copyright 2022, AAAS. E) SEM image of an algal microrobot (pseudocolored green, *C. reinhardtii*). 2D propulsion trajectories of the algae microrobots under a uniform field. Reproduced with permission.^[129] Copyright 2018, WILEY-VCH GmbH. F) Schematic of acidophilic algae microrobots for *in vivo* delivery applications in GI tract. Acidophilic algae robots are capable of prolonged motion in both neutral and acidic environments, whereas neutrophilic algae are corroded and degraded in highly acidic environments. Reproduced with permission.^[131] Copyright 2022, AAAS.

normal cells. MTBs have been used to transport drug-loaded NLS into hypoxic regions of tumors via their magnetoaerotaxis.^[120] This feature can help MTB-driven microrobots to improve the targeting ratio of drugs to the tumor cells. Meanwhile, the existence of magnetosomes enables MTBs to swim along the external field and precisely navigate to the tumor cells. As the nonpathogenic bacteria in the human body, *E. coli* has been demonstrated to carry microparticles,^[121,122] NLS,^[81] and RBCs^[80,123] for targeted active delivery. Through streptavidin-biotin binding,

the bacterial membrane can be connected with the RBC membrane, magnetic nanoparticles, or NLS. Apart from the above linking manner, the bacterial membrane can also be attached to the surface of synthetic microparticles through electrostatic interaction,^[121,124] hydrophobic interaction,^[125,126] and carbodiimide chemistry.^[127,128] The magnetic guidance ability can be achieved by embedding magnetic nanoparticles into microparticles and RBCs or directly linking magnetic nanoparticles with the membrane of bacteria. The anticancer drug model,

DOX, can be encapsulated into RBCs to minimize the leakage during the delivery process and released when exposed to pH or NIR light. Akolpoglu et al. proposed *E. coli*-driven microrobots capable of colonizing tumor spheroids for on-demand release of the drug molecules^[81] (see Figure 7D). NLs carrying DOX and photothermal agents, indocyanine green (ICG), which enable the release of DOX by NIR stimulus, are attached to *E. coli* through streptavidin-biotin binding. The excellent swimming ability of *E. coli* allows microrobots to navigate through biological matrices, which is promising for drug delivery in viscoelastic and solid environments.

Microalgae have been demonstrated to possess natural biodegradability and desirable cytotoxicity in physiological environments.^[25] The fabrication procedure of algal microrobots is facile, cost effective, and fast. The negatively charged algae membrane can assemble with the positively functionalized magnetic polystyrene particles,^[129] as shown in Figure 7E. The magnetic polystyrene particles are deposited with a positively charged polyelectrolyte layer, which can enhance the adhesion of bacteria to the microparticles through strong electrostatic interactions.^[121] Moreover, the existence of magnetic polystyrene particles ascertains the maneuverability of algal microrobots under a magnetic field. The fluorescent isothiocyanate-labeled dextran is loaded into magnetic polystyrene particles and delivered to HeLa cells as a proof-of-concept active cargo delivery demonstration. The proposed targeted drug delivery is realized by injecting drug-loaded microrobots near lesions. Oral delivery to the GI tract has been utilized in the last decades because of its high patient compliance, noninvasiveness, and low cost. The microrobotic-based capsule toward oral delivery in the GI tract is restricted by the short propulsion lifetime. Natural algae with the advantage of fast and long-lasting swimming performance can effectively address this limitation. Zhang et al.^[130] reported an efficient algal microrobotic system, where fluorescent dye or cell membrane-coated nanoparticle-functionalized algal microrobots are embedded inside a pH-responsive capsule. The capsule layer can protect algal microrobots from harsh gastric environments in the stomach. Upon the release from the capsule, the algal microrobots swim in the intestinal fluid for more than 12 h and release the carried DOX to treat GI diseases. Zhang et al.^[131] also harnessed acidophilic microalgae, *Chlamydomonas pitschmannii* (*C. pitschmannii*), to construct biohybrid microrobotic system toward GI delivery applications, as shown in Figure 7F. *C. pitschmannii* shows a remarkable swimming ability even in acidic environments (pH < 4) and maintains its swimming speed for long time periods. Thus, this ability enables *C. pitschmannii* to pass through the GI tract with the low pH condition. The algal microrobots are fabricated by combining the acidophilic microalgae with RBC membrane-coated nanoparticles that load a green fluorescent dye. The long-time retention of fluorescent signals in both the stomach and the small intestine validates the microrobots based on *C. pitschmannii* which can help to improve chemotherapeutic performance in the GI tract. Due to the maneuverability of soft bio-microrobots, they can be directed by external stimuli to transport cargo to specific positions. The cargo is released and takes effect after reaching the targeted location, thereby improving targeted efficiency compared with systemic administration. In addition, their small size enables

them to access hard-to-reach locations in the human body, which holds the potential for microsurgery with minimal trauma.

4.2. Surgery

Large surgical tools can be teleoperated by a clinician, yet are not able to arrive at hard-to-reach positions in the human body. Due to the microscale size, the microrobotic systems make it possible to remotely interfere in the circulatory system, the urinary system, and the central nervous system with tiny passages.^[132] In ocular medicine, the molecule passively diffuses in the eye. However, the diffusion is hampered by the tight macromolecular matrix in the vitreous. Wu et al.^[133] reported magnetically helical microrobots with a perfluorocarbon surface coating that minimizes the interaction of the microrobots with the macromolecular network in the vitreous. The microrobots swarm penetrates the tight macromolecular matrix of the porcine vitreous and reaches the retina within 30 min under the magnetic field. Standard optical coherence tomography is used to visualize the microrobots swarm and send feedback on the position to the user. The alternative potential strategy for surgery is to combine large surgical tools, such as endoscopy, and untethered microrobots. The endoscopy enables rapid deployment and long-distance delivery across organs and tissue, while microrobots can access the deep regions within tortuous ducts, such as tympanostomy tube^[134] and bile duct,^[135,136] that are difficult to reach with the endoscope. Therefore, microrobotic systems open a new avenue for surgery.

4.2.1. Biopsy

A biopsy is a medical procedure that takes a small sample of body tissue for further histological, cytological, or genetic examination. Biopsies are required in a wide range of organs including the liver, breast, lung, and skin. Untethered microgrippers can achieve the retrieval of an object from a far location owing to their grasping capability. The thermochemically triggered microgrippers have been demonstrated to capture clusters of live fibroblast cells without damaging the cell viability.^[35] The in vitro biopsy has been performed on a tissue sample from a bovine bladder as well. The enzymatically triggered microgrippers can carry the cells without destroying RNA structure.^[36] Afterward, Gultepe et al. demonstrated ex vivo tissue excision of a porcine liver and in vivo tissue retrieval from a porcine biliary tree using thermally responsive untethered microgrippers.^[137] The high-quality RNA and DNA from the retrieved tissue can be utilized to undertake diagnostics. A single-cell manipulation is crucial for biosensing, surgery, robotics, and cell analysis. Jin et al.^[138] exploited a thermally responsive wax layer to fabricate untethered microgrippers to actively capture or excise single cells in a biocompatible manner. Wax is chemically and biologically inert and biocompatible and widely used in food products, as well as displays a range of phase transition temperatures of relevance to biology and the human body. Therefore, this microgripper does no harm to the human body when performing the biopsy. Figure 8A includes the optical microscopy images that show the process of a microgripper capturing and excising cells from

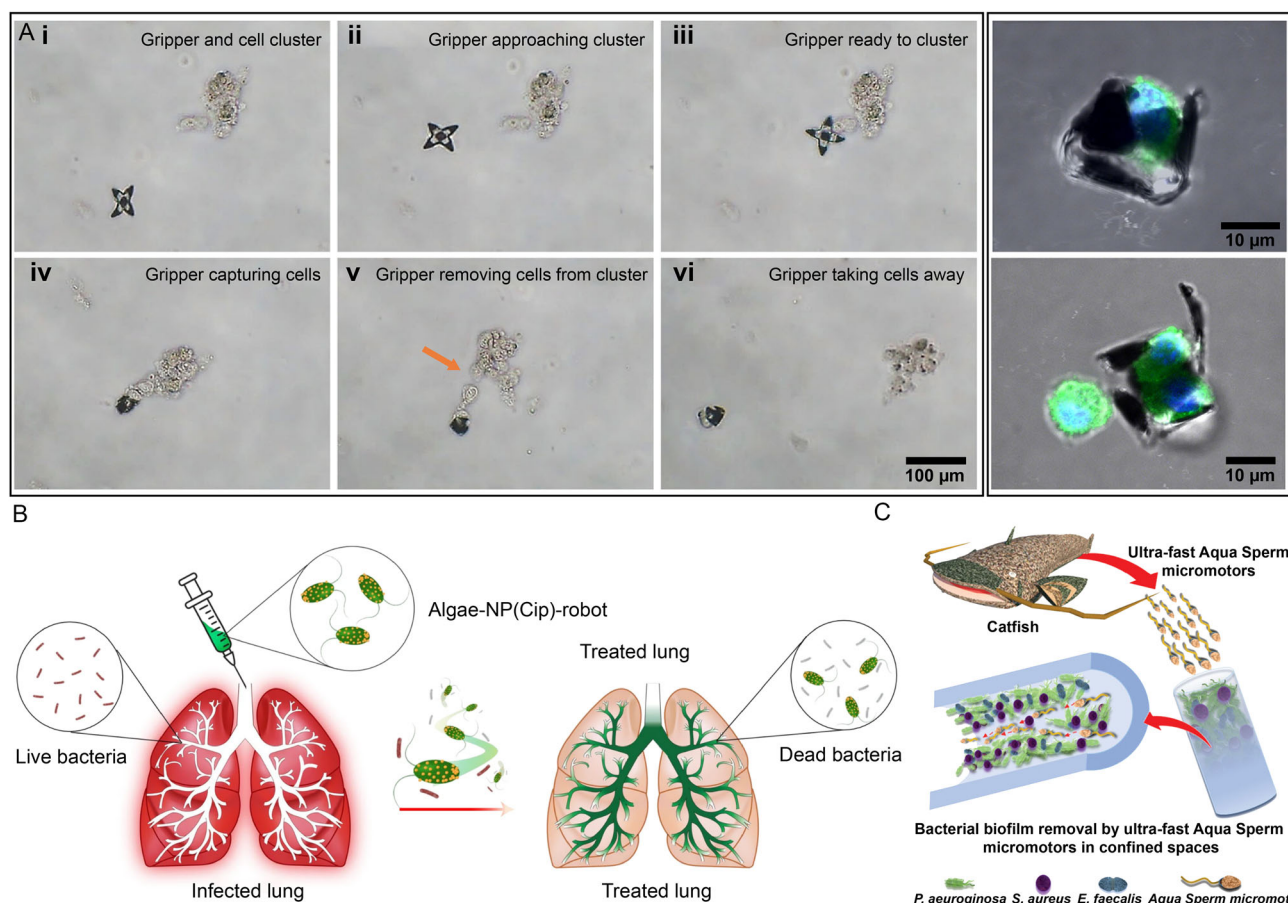


Figure 8. Surgical applications including biopsy and biofilm eradication of soft bio-microbots. (A) Optical microscopy images (i)–(vi) show the process of a microgripper capturing and excising cells from a cell cluster. Immunofluorescence images exhibit suspended fibroblast cells captured by the grippers, including single-cell and two-cell captures. Reproduced with permission.^[138] Copyright 2020, American Chemical Society. (B) Schematic depicting the utilization of algal microrobots for the treatment of a bacterial lung infection. Reproduced with permission.^[130] Copyright 2022, Springer Nature. (C) Schematic representation of sperm microrobots destroying three species of bacterial biofilm colonized on medical and laboratory tubing. Reproduced with permission.^[144] Copyright 2021, Wiley-VCH GmbH.

a cell cluster and the immunofluorescence images that display single cell and two cell captured by the microgripper.

4.2.2. Biofilm Eradication

Biofilms are a cluster of aggregates of bacterial cells encased in a matrix of extracellular polymeric. The extracellular polymeric substances (EPS) protect bacterial cells from hostile environments, antibiotics, or the immune systems of host organisms.^[139] Biofilms are ubiquitous in industrial settings, such as sewage treatment, bioleaching, and the food industry. One of the most commonly used methods for treating clinical bacterial infections is the administration of antibiotics. However, this approach is ineffective because the antibiotics randomly circulate in biological fluids and may be blocked by EPS. Microbots provide a feasible method for targeted drug delivery to eradicate biofilms due to the capability of penetrating the matrix owing to their size and propulsive thrust.^[140] Stanton et al.^[141] exploited the nonpathogenic MTB to integrate with antibiotics-loaded microtubes to establish a controllable microrobotic system

capable of targeting an infectious biofilm. The microbots can respond to the external magnetic field and reach the biofilm. Unlike bacteria-driven microrobotic systems facing potential pathogenicity or immunogenicity, algal microrobotic systems allow on-demand biofilm eradication in a safer way. Shchelik et al.^[142] leveraged the surface engineering of microalgae to fabricate an antibiotics-loaded biohybrid microrobotic system. The antibiotics are conjugated to the microalgae surface via click chemistry. The direct control of algal microrobots is demonstrated using the phototactic properties of the cells. To avoid the immune clearance of soft bio-microbots by alveolar macrophages, Zhang et al.^[143] created algal microrobots by attaching antibiotic-loaded neutrophil membrane-coated polymeric nanoparticles to natural microalgae. The neutrophil membrane can shield microalgae from the immune system and enable specific binding with target pathogens. Figure 8B depicts the utilization of algal microrobots for the treatment of a bacterial lung infection. Besides, Mayorga-Martinez et al.^[144] found catfish sperm can penetrate and disturb three species of bacterial biofilms colonized on medical and laboratory tubing through mechanical

removal, as shown in Figure 8C. Using their ultrafast speed, the biofilms can be destroyed in a short time. Sperm cells have also been proven to possess the ability to overcome time-periodic interaction force,^[145] which makes them promising for penetrating the EPS of biofilms. Sperm-driven microrobots are a promising option for overcoming biological barriers. However, the maneuverability and propulsive thrust of these sperm-driven microrobots when facing these barriers are yet to be demonstrated.

5. Challenges

Living microorganisms and cells display remarkable swimming abilities due to their soft flagella, serving as a classic illustration of movement in the low-Re regime. Motile microorganisms and cells can provide motility and possess cell membranes with good adhesion to accessories, such as polymeric materials, RBCs, or NLs, which allow for drug loading and prevent release during delivery to the target position. The functional materials enable biohybrid soft microrobots to execute biomedical tasks. On the other hand, flexible materials have been widely used to fabricate synthetic soft microrobots to mimic the motion of the flagellum or replicate the gripping abilities of human hands. Biologically inspired and biohybrid microrobots are two categories of soft bio-microrobots. The summary of soft bio-microrobots has shown their potential to advance minimally invasive medicine, such as targeted delivery and surgery. Nevertheless, there is still a long way from the translation to clinical applications. Great challenges hindering the development of soft bio-microrobots still exist.

Safety is the most important issue for soft bio-microrobots used for *in vivo* applications. As foreign materials, soft bio-microrobots should be removed from the body after completing their biomedical tasks. However, the postapplication retrieval or resorbability of soft bio-microrobots has not been considered and presented in most research. Hence, the fully biodegradable soft bio-microrobots can be a major advancement toward clinical trials. After soft bio-microrobots complete the designated mission in the body, their degradation into nontoxic byproducts will greatly minimize the risk of potential inflammation and other complication, as well as reduce the postoperative recovery time. The incorporation of magnetic materials for directional control of soft bio-microrobots is common in the fabrication process. These magnetic materials typically include magnetic metal layers or magnetic nanoparticles. Although an iron and platinum bilayer can be noncytotoxic and biocompatible after an annealing step,^[146] it cannot be absorbed or metabolized in the human body. It has been shown that magnetic metal layers such as nickel and cobalt are detrimental to tissues and cells. In addition, the strong stiffness of the metal layer used in soft bio-microrobots could result in scratching or harm to healthy tissue or cells during movement. In addition, the resorbability of magnetic nanoparticles depends on their size. The magnetic nanoparticles smaller than 10 nm can be resorbed through renal clearance within a few days, whereas those larger than 100 nm are slowly removed by the spleen and the liver.^[116] Therefore, synthetic material should be evolved to possess biocompatibility and biodegradability in the future. Besides, the selection of

microorganisms and cells for biohybrid soft microrobots must consider their safety in the human body. Researchers have harnessed nonpathogenic microorganism species to create biohybrid microrobots, but an approach to avoid detection by the immune system is often lacking. Commensal bacteria found in the human body can be used to construct biohybrid microrobots, as the commensal bacterial physiology is related to the host behavior and they can evade the clearance of the immune system in the host. In the future, commensal bacteria species or microorganisms with cell-mimicking properties could be a viable choice to fabricate biohybrid microrobots for precision nanomedicine. Overall, the complexity of cellular and organismal immune response to the bio-microrobots remains to be studied beyond cytotoxicity of the involved materials.

The design and manufacture of soft bio-microrobots are specific to each biomedical application, so there is not a single generic soft bio-microrobot for all applications. Considering varying conditions in the human body, soft bio-microrobots must adapt to the complex conditions in the specific organs or cells. Therefore, a strategic method should be given to guide the design of soft bio-microrobots based on the specific application scenario. For example, the soft bio-microrobots aiming for GI delivery should be able to withstand the acid environments in the stomach. Also, when soft bio-microrobots are utilized in the field of ocular medicine, they need to penetrate through the tight macromolecular matrix in the vitreous. To this end, soft bio-microrobots with the ability to penetrate should be designed, which is also crucial for reaching tumor tissues and bacterial cells in biofilms. Meanwhile, the fabrication method should satisfy the requirement of simplicity, cost-effectiveness, and high productivity. In the future, a facile and reliable fabrication method should be developed to mass produce soft bio-microrobots. The architecture of soft bio-robotics will develop toward microrobot intelligence. Soft bio-robotics will have control systems to control other components, such as power components, interactive components, and functional components. The construction of these components will enable the invention of intelligent microrobots to perform more complex tasks than biomedical applications, for example, data storage and data processing. However, more advanced components that are gifted with perception and intelligence need the development of micro-/nanofabrication techniques.^[147]

As the human body is the target environment for most soft bio-microrobots, they must have the ability to adapt to complicated conditions and maintain long-term motility in the human body. The motion and navigation of soft bio-microrobots in physiological environments can be impacted by the presence of proteins, lipids, nucleic acids, high ionic strength, and varying pH levels. Furthermore, the movement of soft bio-microrobots in non-Newtonian and inhomogeneous physiological fluids remains uncertain due to their complex properties. The challenge of overcoming biological barriers such as biofouling, blood flow, the blood–brain barrier, and cell membranes is also yet to be fully addressed. In precision nanomedicine, the therapeutic drugs need to enter the cell to exert on the nuclei or cytosol of cells. The cell membrane, comprising a phospholipid bilayer, proteins, and polysaccharides, can act as a barrier by preventing the entry of drug-loaded soft bio-microrobots into cells. The surface of soft bio-microrobots is absorbed by plasma protein and

identified by mononuclear phagocytic cells of the reticuloendothelial system in the blood vessel,^[148] leading to their removal from the bloodstream. Maintaining long-term and exceptional motility in the body remains a substantial challenge for soft bio-microrobots.

Microorganisms and cells have been a major inspiration for the development of soft bio-microrobots. Nevertheless, the current soft bio-microrobots lack the ability to sense and respond to surrounding environments, as seen in many microorganisms and cells. Those abilities are known as chemotaxis, magnetotaxis, phototaxis, rheotaxis, and thermotaxis. For instance, MTBs and microalgae can respond to the external magnetic field and light illumination, respectively. Sperm cells can navigate toward the ovum primarily through rheotaxis, thermotaxis, and chemotaxis. Although the swimming ability of current biohybrid soft microrobots is comparable with that of the microorganism and cell, the inherent abilities of microorganisms and cells are not well explored and harnessed in biomedical applications. Replicating the structure of microorganisms and cells is only the first step, these tactic behaviors should be implemented into soft bio-microrobots to realize real biomimetics engineering.

Soft bio-microrobot swarms can improve the targeting efficacy and carry a larger amount of drugs to treat diseases. Moreover, the aggregation of soft bio-microrobots will be easier to be tracked in vivo compared to one single microrobot. In microrobotic systems, the tracking precision affects the implementation of the control algorithm and the precision control of microrobots in the human body. Currently, tracking a microrobot inside the human body is still a grand challenge because of the limited resolution, penetration depth, or adverse effects of current imaging techniques.^[149] Therefore, developing soft bio-microrobot swarms can not only improve drug targeting efficiency but also lower the difficulty of tracking. However, the collective behavior of soft bio-microrobots is complicated because it involves complex interaction with the fluidic environments, external field, surrounding microrobots, and adjacent soft bio-microrobots. In the future, the underlying mechanism needs to be understood to develop soft bio-microrobot swarms with advanced functions and explore their adaptability in complex environments.

6. Conclusions

This review summarizes the state-of-the-art of soft bio-microrobots for targeted cargo delivery and surgery. Limited by the size of microrobots, batteries are not a suitable power source as the deliverable energy scales with volume. By converting the power of external fields or utilizing the self-propulsion of microorganisms or cells, soft bio-microrobots are capable of swimming in the low-Re regime. The functional components of soft bio-microrobots enable them to be guided, respond to the surrounding environments, and execute in vivo biomedical tasks. The development of soft bio-microrobots is shifting from mimicking the swimming ability of creatures to endowing them with the same characteristics as creatures. The future of soft bio-microrobots must move toward simplicity, safety, adaptability, and intelligence. Although there is still a considerable journey ahead for clinical application, soft bio-microrobots with the above properties will advance minimally invasive medicine and revolutionize human life in the future.

Acknowledgements

Z.W. thanks financial support of the China Scholarship Council under grant no. 202006120058. This work was also supported by the European Research Council (ERC) under the European Union's Horizon 2020 Research and Innovation programme under grant 866494 project-MAESTRO.

Conflict of Interest

The authors declare no conflict of interest.

Data Availability Statement

Research data are not shared.

Keywords

actuation mechanisms, biomimetics, microorganisms, soft bio-microrobots, targeted delivery

Received: February 16, 2023

Revised: April 20, 2023

Published online: June 29, 2023

- [1] J. Amend, N. Cheng, S. Fakhouri, B. Culley, *Soft Robotics* **2016**, 3, 213.
- [2] G. Li, X. Chen, F. Zhou, Y. Liang, Y. Xiao, X. Cao, Z. Zhang, M. Zhang, B. Wu, S. Yin, Y. Xu, H. Fan, Z. Chen, W. Song, W. Yang, B. Pan, J. Hou, W. Zou, S. He, X. Yang, G. Mao, Z. Jia, H. Zhou, T. Li, S. Qu, Z. Xu, Z. Huang, Y. Luo, T. Xie, J. Gu, S. Zhu, W. Yang, *Nature* **2021**, 591, 66.
- [3] K. C. Galloway, K. P. Becker, B. Phillips, J. Kirby, S. Licht, D. Tchernov, R. J. Wood, D. F. Gruber, *Soft Robotics* **2016**, 3, 23.
- [4] Y. Kim, E. Genevriere, P. Harker, J. Choe, M. Balicki, R. W. Regenerhardt, J. E. Vranic, A. A. Dmytriw, A. B. Patel, X. Zhao, *Science Robotics* **2022**, 7, eabg9907.
- [5] W. Hu, G. Z. Lum, M. Mastrangeli, M. Sitti, *Nature* **2018**, 554, 81.
- [6] M. Sun, C. Tian, L. Mao, X. Meng, X. Shen, B. Hao, X. Wang, H. Xie, L. Zhang, *Advanced Functional Materials* **2022**, 32, 2112508.
- [7] S. Palagi, A. G. Mark, S. Y. Reigh, K. Melde, T. Qiu, H. Zeng, C. Parmeggiani, D. Martella, A. Sanchez-Castillo, N. Kapernaum, F. Giesselmann, D. S. Wiersma, E. Lauga, P. Fischer, *Nat. Mater.* **2016**, 15, 647.
- [8] S.-J. Park, M. Gazzola, K. S. Park, S. Park, V. Di Santo, E. L. Blevins, J. U. Lind, P. H. Campbell, S. Dauth, A. K. Capulli, F. S. Pasqualini, S. Ahn, A. Cho, H. Yuan, B. M. Maoz, R. Vijaykumar, J.-W. Choi, K. Deisseroth, G. V. Lauder, L. Mahadevan, K. K. Parker, *Science* **2016**, 353, 158.
- [9] N. Kellaris, V. Gopaluni Venkata, G. M. Smith, S. K. Mitchell, C. Keplinger, *Science Robotics* **2018**, 3, eaar3276.
- [10] E. Acome, S. K. Mitchell, T. Morrissey, M. Emmett, C. Benjamin, M. King, M. Radakovitz, C. Keplinger, *Science* **2018**, 359, 61.
- [11] A. G. Athanassiadis, Z. Ma, N. Moreno-Gomez, K. Melde, E. Choi, R. Goyal, P. Fischer, *Chem. Rev.* **2021**, 122, 5165.
- [12] J. Li, C. C. Mayorga-Martinez, C.-D. Ohl, M. Pumera, *Adv. Funct. Mater.* **2022**, 32, 2102265.
- [13] E. M. Purcell, *Am. J. Phys.* **1977**, 45, 3.
- [14] E. Lauga, T. R. Powers, *Rep. Prog. Phys.* **2009**, 72, 096601.
- [15] E. H. Harris, *Annu. Rev. Plant Biol.* **2001**, 52, 363.

- [16] E. Gaffney, H. Gadêlha, D. Smith, J. Blake, J. Kirkman-Brown, *Annu. Rev. Fluid Mech.* **2011**, 43, 501.
- [17] Y. Kim, H. Yuk, R. Zhao, S. A. Chester, X. Zhao, *Nature* **2018**, 558, 274.
- [18] S. R. Dabbagh, M. R. Sarabi, M. T. Birtek, S. Seyfi, M. Sitti, S. Tasoglu, *Nature Communications* **2022**, 13, 5875.
- [19] M. Wehner, R. L. Truby, D. J. Fitzgerald, B. Mosadegh, G. M. Whitesides, J. A. Lewis, R. J. Wood, *Nature* **2016**, 536, 451.
- [20] R. F. Shepherd, F. Ilievski, W. Choi, S. A. Morin, A. A. Stokes, A. D. Mazzeo, X. Chen, M. Wang, G. M. Whitesides, *Proc. Natl. Acad. Sci.* **2011**, 108, 20400.
- [21] Z. Zheng, H. Wang, S. O. Demir, Q. Huang, T. Fukuda, M. Sitti, *Sci. Adv.* **2022**, 8, eade6135.
- [22] W. Gao, S. Sattayasamitsathit, K. M. Manesh, D. Weihs, J. Wang, *J. Am. Chem. Soc.* **2010**, 132, 14403.
- [23] V. Magdanz, J. Gebauer, D. Mahdy, J. Simmchen, I. S. M. Khalil, In *International Conference on Manipulation, Automation and Robotics at Small Scales (MARSS)*. IEEE, Helsinki, Finland, **2019**, 1–6.
- [24] W. Gao, X. Feng, A. Pei, C. R. Kane, R. Tam, C. Hennessy, J. Wang, *Nano Lett.* **2014**, 14, 305.
- [25] X. Yan, Q. Zhou, M. Vincent, Y. Deng, J. Yu, J. Xu, T. Xu, T. Tang, L. Bian, Y.-X. J. Wang, K. Kostarelos, L. Zhang, *Sci. Robotics* **2017**, 2, eaaq1155.
- [26] Y. Dong, L. Wang, N. Xia, Z. Yang, C. Zhang, C. Pan, D. Jin, J. Zhang, C. Majidi, L. Zhang, *Sci. Adv.* **2022**, 8, eabn8932.
- [27] V. Magdanz, S. Sanchez, O. G. Schmidt, *Adv. Mater.* **2013**, 25, 6581.
- [28] B. Behkam, M. Sitti, *Appl. Phys. Lett.* **2007**, 90, 023902.
- [29] F. Zhang, Z. Li, L. Yin, Q. Zhang, N. Askarinam, R. Mundaca-Urbe, F. Tehrani, E. Karshalev, W. Gao, L. Zhang, J. Wang, *J. Am. Chem. Soc.* **2021**, 143, 12194.
- [30] S. Palagi, P. Fischer, *Nat. Rev. Mater.* **2018**, 3, 113.
- [31] L. Ricotti, B. Trimmer, A. W. Feinberg, R. Raman, K. K. Parker, R. Bashir, M. Sitti, S. Martel, P. Dario, A. Menciassi, *Sci. Robotics* **2017**, 2, eaaq0495.
- [32] E. Gultepe, S. Yamanaka, K. E. Laflin, S. Kadam, Y. Shim, A. V. Olaru, B. Limketkai, M. A. Khashab, A. N. Kalloo, D. H. Gracias, *Gastroenterology* **2013**, 144, 691.
- [33] K. Malachowski, M. Jamal, Q. Jin, B. Polat, C. J. Morris, D. H. Gracias, *Nano Lett.* **2014**, 14, 4164.
- [34] J. S. Randhawa, T. G. Leong, N. Bassik, B. R. Benson, M. T. Jochmans, D. H. Gracias, *J. Am. Chem. Soc.* **2008**, 130, 17238.
- [35] T. G. Leong, C. L. Randall, B. R. Benson, N. Bassik, G. M. Stern, D. H. Gracias, *Proc. Nat. Acad. Sci.* **2009**, 106, 703.
- [36] N. Bassik, A. Brafman, A. M. Zarafshar, M. Jamal, D. Luvsanjav, F. M. Selaru, D. H. Gracias, *J. Am. Chem. Soc.* **2010**, 132, 16314.
- [37] S. Fusco, M. S. Sakar, S. Kennedy, C. Peters, R. Bottani, F. Starsich, A. Mao, G. A. Sotiriou, S. Pané, S. E. Pratsinis, D. Mooney, B. J. Nelson, *Adv. Mater.* **2014**, 26, 952.
- [38] C. Yoon, R. Xiao, J. Park, J. Cha, T. D. Nguyen, D. H. Gracias, *Smart Mater. Struct.* **2014**, 23, 094008.
- [39] J. C. Breger, C. Yoon, R. Xiao, H. R. Kwag, M. O. Wang, J. P. Fisher, T. D. Nguyen, D. H. Gracias, *ACS Appl. Mater. Interfaces* **2015**, 7, 3398.
- [40] T. Mirkovic, M. L. Foo, A. C. Arsenault, S. Fournier-Bidoz, N. S. Zacharia, G. A. Ozin, *Nat. Nanotechnol.* **2007**, 2, 565.
- [41] W. Gao, K. M. Manesh, J. Hua, S. Sattayasamitsathit, J. Wang, *Small* **2011**, 7, 2047.
- [42] W. F. Paxton, K. C. Kistler, C. C. Olmeda, A. Sen, S. K. St. Angelo, Y. Cao, T. E. Mallouk, P. E. Lammert, V. H. Crespi, *J. Am. Chem. Soc.* **2004**, 126, 13424.
- [43] B. Jang, E. Gutman, N. Stucki, B. F. Seitz, P. D. Wendel-Garca, T. Newton, J. Pokki, O. Ergeneman, S. Pané, Y. Or, B. J. Nelson, *Nano Lett.* **2015**, 15, 4829.
- [44] D. Ahmed, T. Baasch, B. Jang, S. Pane, J. Dual, B. J. Nelson, *Nano Lett.* **2016**, 16, 4968.
- [45] J. Gray, *J. Exp. Biol.* **1933**, 10, 88.
- [46] T. Li, J. Li, H. Zhang, X. Chang, W. Song, Y. Hu, G. Shao, E. Sandraz, G. Zhang, L. Li, J. Wang, *Small* **2016**, 12, 6098.
- [47] X. Hu, I. C. Yasa, Z. Ren, S. R. Goudou, H. Ceylan, W. Hu, M. Sitti, *Sci. Adv.* **2021**, 7, eabe8436.
- [48] T. Li, J. Li, K. I. Morozov, Z. Wu, T. Xu, I. Rozen, A. M. Leshansky, L. Li, J. Wang, *Nano Lett.* **2017**, 17, 5092.
- [49] S. S. Suarez, A. Pacey, *Hum. Reprod. Update* **2006**, 12, 23.
- [50] R. Dreyfus, J. Baudry, M. L. Roper, M. Fermigier, H. A. Stone, J. Bibette, *Nature* **2005**, 437, 862.
- [51] B. J. Williams, S. V. Anand, J. Rajagopalan, M. T. A. Saif, *Nat. Commun.* **2014**, 5, 1.
- [52] I. S. M. Khalil, H. C. Dijkslag, L. Abelman, S. Misra, *Appl. Phys. Lett.* **2014**, 104, 223701.
- [53] S. Mohanty, U. Siciliani de Cumis, M. Solsona, S. Misra, *AIP Adv.* **2019**, 9, 035352.
- [54] M. Kaynak, A. Ozcelik, A. Nourhani, P. E. Lammert, V. H. Crespi, T. J. Huang, *Lab on a Chip* **2017**, 17, 395.
- [55] I. S. M. Khalil, A. Fatih Tabak, A. Klingner, M. Sitti, *Appl. Phys. Lett.* **2016**, 109, 033701.
- [56] L. Liu, M. Liu, Y. Su, Y. Dong, W. Zhou, L. Zhang, H. Zhang, B. Dong, L. Chi, *Nanoscale* **2015**, 7, 2276.
- [57] J. Xue, T. Wu, Y. Dai, Y. Xia, *Chem. Rev.* **2019**, 119, 5298.
- [58] V. Magdanz, M. Medina-Sánchez, L. Schwarz, H. Xu, J. Elgeti, O. G. Schmidt, *Adv. Mater.* **2017**, 29, 1606301.
- [59] O. G. Schmidt, K. Eberl, *Nature* **2001**, 410, 168.
- [60] I. S. M. Khalil, V. Magdanz, S. Sanchez, O. G. Schmidt, S. Misra, *J. Micro-Bio Robot.* **2014**, 9, 79.
- [61] V. Magdanz, M. Guix, F. Hebenstreit, O. G. Schmidt, *Adv. Mater.* **2016**, 28, 4084.
- [62] H. Xu, M. Medina-Sánchez, O. G. Schmidt, *Angew. Chem. Int. Ed.* **2020**, 59, 15029.
- [63] G. Huszar, C. C. Ozenci, S. Cayli, Z. Zavaczki, E. Hansch, L. Vigue, *Fertil. Steril.* **2003**, 79, 1616.
- [64] M. Medina-Sánchez, L. Schwarz, A. K. Meyer, F. Hebenstreit, O. G. Schmidt, *Nano Lett.* **2016**, 16, 555.
- [65] C. Ridzewski, M. Li, B. Dong, V. Magdanz, *ACS App. Bio Mater.* **2020**, 3, 1616.
- [66] F. Rajabasadi, S. Moreno, K. Fichna, A. Aziz, D. Appelhans, O. G. Schmidt, M. Medina-Sánchez, *Adv. Mater.* **2022**, 34, 2204257.
- [67] C. Chen, X. Chang, P. Angsantikul, J. Li, B. Esteban-Fernández de Ávila, E. Karshalev, W. Liu, F. Mou, S. He, R. Castillo, Y. Liang, J. Guan, L. Zhang, J. Wang, *Adv. Biosyst.* **2018**, 2, 1700160.
- [68] V. Magdanz, I. S. M. Khalil, J. Simmchen, G. P. Furtado, S. Mohanty, J. Gebauer, H. Xu, A. Klingner, A. Aziz, M. Medina-Sánchez, O. G. Schmidt, S. Misra, *Sci. Adv.* **2020**, 6, eaba5855.
- [69] I. S. M. Khalil, V. Magdanz, J. Simmchen, A. Klingner, S. Misra, *Appl. Phys. Lett.* **2020**, 116, 063702.
- [70] K. I. Middelhoeck, V. Magdanz, L. Abelman, I. S. M. Khalil, *Biomed. Mater.* **2022**, 17, 065001.
- [71] Y. Alapan, O. Yasa, B. Yigit, I. C. Yasa, P. Erkoç, M. Sitti, *Annu. Rev. Control Robot Auton. Syst.* **2019**, 2, 205.
- [72] E. Lauga, *Annu. Rev. Fluid Mech.* **2016**, 48, 105.
- [73] R. W. Carlsen, M. R. Edwards, J. Zhuang, C. Pacoret, M. Sitti, *Lab on a Chip* **2014**, 14, 3850.
- [74] J. Zhuang, R. Wright Carlsen, M. Sitti, *Scientific Reports* **2015**, 5, 11403.
- [75] D. Kim, A. Liu, E. Diller, M. Sitti, *Biomed. Microdevices* **2012**, 14, 1009.
- [76] E. Steager, C.-B. Kim, J. Patel, S. Bith, C. Naik, L. Reber, M. J. Kim, *Appl. Phys. Lett.* **2007**, 90, 263901.
- [77] H. C. Berg, D. A. Brown, *Nature* **1972**, 239, 500.

- [78] M. M. Stanton, J. Simmchen, X. Ma, A. Miguel-López, S. Sánchez, *Adv. Mater. Interfaces* **2016**, 3, 1500505.
- [79] M. M. Stanton, B.-W. Park, A. Miguel-López, X. Ma, M. Sitti, S. Sánchez, *Small* **2017**, 13, 1603679.
- [80] Y. Alapan, O. Yasa, O. Schauer, J. Giltinan, A. F. Tabak, V. Sourjik, M. Sitti, *Sci. Robotics* **2018**, 3, eaar4423.
- [81] M. B. Akolpoglu, Y. Alapan, N. O. Dogan, S. F. Baltaci, O. Yasa, G. Aybar Tural, M. Sitti, *Sci. Adv.* **2022**, 8, eabo6163.
- [82] C. T. Lefèvre, D. A. Bazylinski, *Microbiol. Mol. Biol. Rev.* **2013**, 77, 497.
- [83] S. Martel, M. Mohammadi, O. Felfoul, Z. Lu, P. Pouponneau, *Int. J. Robot. Res.* **2009**, 28, 571.
- [84] S. Martel, M. Mohammadi, In *Proc. of the IEEE Inter. Conf. on Robotics and Automation (ICRA)*. IEEE, Anchorage, AK, **2010**, 500–505.
- [85] D. De Lanauze, O. Felfoul, J.-P. Turcot, M. Mohammadi, S. Martel, *Int. J. Robotics Res.* **2014**, 33, 359.
- [86] I. S. M. Khalil, M. P. Pichel, L. Abelman, S. Misra, *Int. J. Robotics Res.* **2013**, 32, 637.
- [87] T. Gwisai, N. Mirkhani, M. G. Christiansen, T. T. Nguyen, V. Ling, S. Schuerle, *Sci. Robotics* **2022**, 7, eabo0665.
- [88] D. B. Weibel, P. Garstecki, D. Ryan, W. R. DiLuzio, M. Mayer, J. E. Seto, G. M. Whitesides, *Proc. Natl. Acad. Sci.* **2005**, 102, 11963.
- [89] G. Santomauro, A. V. Singh, B.-W. Park, M. Mohammadrahimi, P. Erkoc, E. Goering, G. Schütz, M. Sitti, J. Bill, *Adv. Biosyst.* **2018**, 2, 1800039.
- [90] S. Xie, N. Jiao, S. Tung, L. Liu, *Biomed. Microdevices* **2016**, 18, 47.
- [91] M. B. Akolpoglu, N. O. Dogan, U. Bozuyuk, H. Ceylan, S. Kizilel, M. Sitti, *Adv. Sci.* **2020**, 7, 2001256.
- [92] Z. Yang, L. Zhang, *Adv. Intell. Syst.* **2020**, 2, 2000082.
- [93] B. J. Nelson, S. Gervasoni, P. W. Chiu, L. Zhang, A. Zemmar, *Proc. IEEE* **2022**, 110, 1028.
- [94] J. Li, X. Li, T. Luo, R. Wang, C. Liu, S. Chen, D. Li, J. Yue, S.-h. Cheng, D. Sun, *Sci. Robotics* **2018**, 3, eaat8829.
- [95] K. B. Yesin, K. Vollmers, B. J. Nelson, *Int. J. Robot. Res.* **2006**, 25, 527.
- [96] L. Zhang, J. J. Abbott, L. Dong, B. E. Kratochvil, D. Bell, B. J. Nelson, *Appl. Phys. Lett.* **2009**, 94, 064107.
- [97] S. Tottori, L. Zhang, F. Qiu, K. K. Krawczyk, A. Franco-Obregón, B. J. Nelson, *Adv. Mater.* **2012**, 24, 811.
- [98] X.-Z. Chen, B. Jang, D. Ahmed, C. Hu, C. De Marco, M. Hoop, F. Mushtaq, B. J. Nelson, S. Pané, *Adv. Mater.* **2018**, 30, 1705061.
- [99] K. E. Peyer, L. Zhang, B. J. Nelson, *Nanoscale* **2013**, 5, 1259.
- [100] S. Mohanty, I. S. M. Khalil, S. Misra, *Proc. Royal Society A* **2020**, 476, 20200621.
- [101] H. Ceylan, J. Giltinan, K. Kozielski, M. Sitti, *Lab on a Chip* **2017**, 17, 1705.
- [102] M. L. Palmeri, A. C. Sharma, R. R. Bouchard, R. W. Nightingale, K. R. Nightingale, *IEEE Trans. Ultrason. Ferroelectr. Freq. Control* **2005**, 52, 1699.
- [103] T. Xu, L.-P. Xu, X. Zhang, *Appl. Mater. Today* **2017**, 9, 493.
- [104] N. Riley, *Ann. Rev. Fluid Mech.* **2001**, 33, 43.
- [105] N. Nama, P.-H. Huang, T. J. Huang, F. Costanzo, *Lab on a Chip* **2014**, 14, 2824.
- [106] D. Ahmed, X. Mao, J. Shi, B. K. Juluri, T. J. Huang, *Lab on a Chip* **2009**, 9, 2738.
- [107] M. Sitti, D. S. Wiersma, *Adv. Mater.* **2020**, 32, 1906766.
- [108] X. Pang, J.-a. Lv, C. Zhu, L. Qin, Y. Yu, *Adv. Mater.* **2019**, 31, 1904224.
- [109] K. Foster, R. Smyth, *Microbiol. Rev.* **1980**, 44, 572.
- [110] J. Gray, G. Hancock, *J. Exp. Biol.* **1955**, 32, 802.
- [111] H. C. Berg, *E. coli in Motion*, Springer, New York, NY **2004**.
- [112] H. C. Berg, *Annu. Rev. Biochem.* **2003**, 72, 19.
- [113] R. Coy, H. Gadêlha, *J. Royal Soc. Interface* **2017**, 14, 20170065.
- [114] R. Cortez, *SIAM J. Sci. Comput.* **2001**, 23, 1204.
- [115] Y. Sowa, R. M. Berry, *Q. Rev. Biophys.* **2008**, 41, 103.
- [116] S. Wilhelm, A. J. Tavares, Q. Dai, S. Ohta, J. Audet, H. F. Dvorak, W. C. Chan, *Nat. Rev. Mater.* **2016**, 1, 16014.
- [117] W. Gao, D. Kagan, O. S. Pak, C. Clawson, S. Campuzano, E. Chuluun-Erdene, E. Shipton, E. E. Fullerton, L. Zhang, E. Lauga, J. Wang, *Small* **2012**, 8, 460.
- [118] H. Xu, M. Medina-Sánchez, V. Magdanz, L. Schwarz, F. Hebenstreit, O. G. Schmidt, *ACS Nano* **2018**, 12, 327.
- [119] H. Xu, M. Medina-Sánchez, W. Zhang, M. P. Seaton, D. R. Brison, R. J. Edmondson, S. S. Taylor, L. Nelson, K. Zeng, S. Bagley, C. Ribeiro, L. P. Restrepo, E. Lucena, C. K. Schmidt, O. G. Schmidt, *Nanoscale* **2020**, 12, 20467.
- [120] O. Felfoul, M. Mohammadi, S. Taherkhani, D. De Lanauze, Y. Zhong Xu, D. Loghin, S. Essa, S. Jancik, D. Houle, M. Lafleur, L. Gaboury, M. Tabrizian, N. Kaou, M. Atkin, T. Vuong, G. Batist, N. Beauchemin, D. Radzioch, S. Martel, *Nat. Nanotechnol.* **2016**, 11, 941.
- [121] B.-W. Park, J. Zhuang, O. Yasa, M. Sitti, *ACS Nano* **2017**, 11, 8910.
- [122] J. Zhuang, B.-W. Park, M. Sitti, *Adv. Sci.* **2017**, 4, 1700109.
- [123] N. Buss, O. Yasa, Y. Alapan, M. B. Akolpoglu, M. Sitti, *APL Bioengineering* **2020**, 4, 026103.
- [124] R. Bos, H. C. Van der Mei, H. J. Busscher, *FEMS Microbiol. Rev.* **1999**, 23, 179.
- [125] S.-Y. Cheng, S. Heilman, M. Wasserman, S. Archer, M. L. Shuler, M. Wu, *Lab on a Chip* **2007**, 7, 763.
- [126] M. R. Edwards, R. Wright Carlsen, M. Sitti, *Applied Physics Letters* **2013**, 102, 143701.
- [127] S. Uthaman, S. Zheng, J. Han, Y. J. Choi, S. Cho, V. D. Nguyen, J.-O. Park, S.-H. Park, J.-J. Min, S. Park, I.-K. Park, *Adv. Healthc. Mater.* **2016**, 5, 288.
- [128] R. Fernandes, M. Zuniga, F. R. Sassine, M. Karakoy, D. H. Gracias, *Small* **2011**, 7, 588.
- [129] O. Yasa, P. Erkoc, Y. Alapan, M. Sitti, *Advanced Materials* **2018**, 30, 1804130.
- [130] F. Zhang, Z. Li, Y. Duan, A. Abbas, R. Mundaca-Urbe, L. Yin, H. Luan, W. Gao, R. H. Fang, L. Zhang, J. Wang, *Sci. Robot.* **2022**, 7, eabo4160.
- [131] F. Zhang, Z. Li, Y. Duan, H. Luan, L. Yin, Z. Guo, C. Chen, M. Xu, W. Gao, R. H. Fang, L. Zhang, J. Wang, *Sci. Adv.* **2022**, 8, eade6455.
- [132] B. J. Nelson, I. K. Kaliakatsos, J. J. Abbott, *Annu. Rev. Biomed. Eng.* **2010**, 12, 55.
- [133] Z. Wu, J. Troll, H.-H. Jeong, Q. Wei, M. Stang, F. Ziemssen, Z. Wang, M. Dong, S. Schnichels, T. Qiu, P. Fischer, *Sci. Adv.* **2018**, 4, eaat4388.
- [134] Y. Dong, L. Wang, Z. Zhang, F. Ji, T. K. Chan, H. Yang, C. P. Chan, Z. Yang, Z. Chen, W. T. Chang, J. Y. K. Chan, J. J. Y. Sung, L. Zhang, *Sci. Adv.* **2022**, 8, eabq8573.
- [135] M. Sun, K. F. Chan, Z. Zhang, L. Wang, Q. Wang, S. Yang, S. M. Chan, P. W. Y. Chiu, J. J. Y. Sung, L. Zhang, *Adv. Mater.* **2022**, 34, 2201888.
- [136] B. Wang, K. F. Chan, K. Yuan, Q. Wang, X. Xia, L. Yang, H. Ko, Y.-X. J. Wang, J. J. Y. Sung, P. W. Y. Chiu, L. Zhang, *Science Robotics* **2021**, 6, eabd2813.
- [137] E. Gultepe, J. S. Randhawa, S. Kadam, S. Yamanaka, F. M. Selaru, E. J. Shin, A. N. Kalloo, D. H. Gracias, *Adv. Mater.* **2013**, 25, 514.
- [138] Q. Jin, Y. Yang, J. A. Jackson, C. Yoon, D. H. Gracias, *Nano Lett.* **2020**, 20, 5383.
- [139] H.-C. Flemming, J. Wingender, *Nat. Rev. Microbiol.* **2010**, 8, 623.
- [140] Z. Zhang, L. Wang, T. K. Chan, Z. Chen, M. Ip, P. K. Chan, J. J. Sung, L. Zhang, *Adv. Healthc. Mater.* **2022**, 11, 2101991.
- [141] M. M. Stanton, B.-W. Park, D. Vilela, K. Bente, D. Faivre, M. Sitti, S. Sánchez, *ACS Nano* **2017**, 11, 9968.
- [142] I. S. Shchelik, J. V. Molino, K. Gademann, *Acta Biomater.* **2021**, 136, 99.

- [143] F. Zhang, J. Zhuang, Z. Li, H. Gong, B. E.-F. de Ávila, Y. Duan, Q. Zhang, J. Zhou, L. Yin, E. Karshalev, W. Gao, V. Nizet, R. H. Fang, L. Zhang, J. Wang, *Nat. Mater.* **2022**, 21, 1324.
- [144] C. C. Mayorga-Martinez, J. Zelenka, J. Grmela, H. Michalkova, T. Ruml, J. Mareš, M. Pumera, *Adv. Sci.* **2021**, 8, 2101301.
- [145] Z. Wang, A. Klingner, V. Magdanz, M. W. Hoppenreijts, S. Misra, I. S. M. Khalil, *Adv. Biol.* **2023**, 7, 2200210.
- [146] V. M. Kadiri, C. Bussi, A. W. Holle, K. Son, H. Kwon, G. Schütz, M. G. Gutierrez, P. Fischer, *Adv. Mater.* **2020**, 32, 2001114.
- [147] T.-Y. Huang, H. Gu, B. J. Nelson, *Annu. Rev. Control Robot Auton. Syst.* **2022**, 5, 279.
- [148] S. Tenzer, D. Docter, J. Kuharev, A. Musyanovych, V. Fetz, R. Hecht, F. Schlenk, D. Fischer, K. Kiouptsi, C. Reinhardt, K. Landfester, H. Schild, M. Maskos, S. K. Knauer, R. H. Stauber, *Nat. Nanotechnol.* **2013**, 8, 772.
- [149] A. Aziz, S. Pane, V. Iacovacci, N. Koukourakis, J. Czarnecki, A. Menciassi, M. Medina-Sánchez, O. G. Schmidt, *ACS Nano* **2020**, 14, 10865.



Zihan Wang obtained his B. Eng. in mechanical and electrical engineering from Wuhan University of Technology in 2018 and his M.Eng. in mechanical engineering from Harbin Institute of Technology in 2020. Currently, he is pursuing his Ph.D. in Biomedical Engineering at University of Groningen and University Medical Center Groningen, The Netherlands. His research interests focus on the fabrication, elasto-hydrodynamics, modeling, and biomedical applications of magnetically biohybrid microrobots.



Anke Klingner received her Diploma and Ph.D. in physics from TU Dresden, Germany, and Ulm University, Germany. For three years she was a researcher and teaching assistant at Ulm University, Germany. She is currently working at German university in Cairo. Her research interests include physical modeling of microrobots, material characterization, fabrication of soft microrobots, and biologically inspired systems.



Veronika Magdanz obtained her Ph.D. from TU Dresden in 2016 for research on sperm-driven microrobots performed at the Leibniz Institute for Solid State and Materials Research IFW Dresden in Germany. Subsequently, she conducted research on sperm and sperm-templated microrobots at the Applied Zoology Department of the TU Dresden. During her time as Humboldt Fellow and La Caixa Junior Leader at the Institute for Bioengineering of Catalonia, Barcelona, she explored medical applications of flexible magnetic small-scale robots and 3D bioprinting. She is currently an assistant professor at the University of Waterloo. Her main research interest is in microrobotics for medical applications and sperm behavior.



Sarthak Misra received his master's degree from McGill University, Canada, and doctoral degree from the Johns Hopkins University, USA, both in mechanical engineering. He is currently a full professor with the Department of Biomechanical Engineering, University of Twente, The Netherlands, and the Department of Biomedical Engineering, University Medical Center Groningen, The Netherlands. Prior to commencing his doctoral studies, he was a dynamics and controls analyst with the International Space Station Program. His research interests include surgical robotics and medical micro-/nanorobotics. He is the recipient of the European Research Council Starting, Proof-of-Concept, and Consolidator Grants and the Netherlands Organization for Scientific Research VENI and VIDI Awards.



Islam S. M. Khalil received his Ph.D. in mechatronics engineering from Sabanci University, in 2011. He became a postdoctoral research associate with the Robotics and Mechatronics research group and Technical Medical Centre (TechMed Centre), University of Twente, Enschede, The Netherlands. In 2014, he became an assistant professor with the Department of Mechatronics, German University, in Cairo, New Cairo, Egypt, where he directed the Medical Micro and Nano Robotics Laboratory. In 2018, he was appointed as an associate professor with the same department. In 2019, he became an assistant professor with the Department of Biomechanical Engineering, University of Twente. His research interests include modeling, design, and control of soft microrobots, biologically inspired systems, motion control systems, mechatronics system design, and untethered magnetic micro-/nanorobotics with applications to micro-/nanomanipulation, magnetic manipulation, and targeted drug delivery.